OSL dating of the Mesolithic site Nilsvikdalen 7, Bjorøy, Norway.

Elin Jirdén

Dissertations in Geology at Lund University,
Master's thesis, no 633
(45 hp/ECTS credits)

Department of Geology
Lund University
2022

OSL dating of the Mesolithic site Nilsvikdalen 7, Bjorøy, Norway.

Master's thesis

Elin Jirdén

Department of Geology
Lund University
2022

Contents

1 Introduction **7**
1.1 Research questions and purpose of study 7
2 Archaeological applications of OSL **7**
3 Regional background **8**
3.1 Geological setting 8
3.2 Archaeological setting 8
3.3 Previous work at the Nilsvikdalen 7 site 9
4 Luminescence dating background **10**
4.1 OSL age calculation factors 11
4.2 The Single Aliquot Regenerative-dose protocol 11
4.3 Quality tests to assure correct age determinations 12
5 Methods **13**
5.1 Field work 13
5.2 OSL sample characteristics and corresponding radiocarbon dates 13
5.3 OSL lab procedure 13
6 Results **16**
6.1 Field work 16
6.2 Luminescence measurements 17
6.2.1 Bleaching test 17
6.2.2 OSL measurements 17
7 Discussion **19**
7.1 Age reliability 19
7.1.1 Reliability of quality tests and equivalent doses 19
7.1.2 Dose rate uncertainties - water content influence 23
7.1.3 Further dose rate considerations 24
7.1.4 Age Model decision 25
7.2 Site Interpretation 26
7.3 Possibilities of future OSL dating at similar sites 27
8 Conclusions **28**
9 Acknowledgements **28**
10 References **29**
Appendix **33**

Cover Picture: At the 2010 excavation of the Nilsvikdalen 7 site. Photo: Leif Inge Åstveit, University of Bergen.

Abstract

ELIN JIRDÉN

Jirdén, E., 2022: OSL dating of the Mesolithic site Nilsvikdalen 7, Bjorøy, Norway. *Dissertations in Geology at Lund University*, No. 633, 34 pp. 45 hp (45 ECTS credits).

Abstract: Luminescence dating is a well-established dating method within geological and archaeological research. However, the use of luminescence dating, and more specifically optically stimulated luminescence (OSL), is currently underutilised in Norwegian archaeology. This study set about determining the suitability of this dating method as a viable option for excavations of Norwegian coastal Stone Age sites. This is done by OSL dating six samples from three superimposed cultural layers at a settlement (Nilsvikdalen 7) at Bjorøy, SW Norway, which has previously been radiocarbon dated to the Late Mesolithic period, and subsequently evaluating the method suitability from the results.

The cultural layers all consist of varying degrees of humus-rich sand with charcoal, where OSL samples were taken from inside and outside an interpreted hut structure. Quartz OSL dating was carried out using the Single Aliquot Regenerative-dose (SAR) protocol for all six samples and yielded successful results. The samples displayed a strong quartz signal with excellent characteristics. The water content of the site yielded the highest uncertainties for the dose rate determination and was after thorough evaluation determined to ~ 63 – 114%. Dose rate was determined to ~ 2 – 4 Gy/ka. Different age models were applied, where the mean age was chosen for the final age determination. The bottom cultural layer was dated to the Late Mesolithic, with OSL ages of 8.07 ± 0.51 ka and 7.02 ± 0.43 ka inside the hut, as well as 6.60 ± 0.40 ka outside the hut boundary. The middle and upper layers were dated to Late Mesolithic – Early Neolithic, where the middle unit displayed an age of 6.25 ± 0.36 ka and the upper layer yielded ages of 5.56 ± 0.32 ka and 6.94 ± 0.36 ka (all dates inside the hut). Three of the samples overlap with the corresponding radiocarbon dates, whilst the other three do not statistically agree (values outside of ± 2 σ) with the radiocarbon dates. For the samples without statistical agreement, the OSL ages produced are younger than the corresponding radiocarbon dates.

For future OSL dating it is suggested to, if possible, take a control sample of recent or known age from a site area to reduce possible uncertainties in the luminescence age determination process. Given the successful dating of the Nilsvikdalen 7 site, this project demonstrates how OSL dating could provide a good solution for future dating of Norwegian coastal Stone Age sites.

Keywords: OSL dating, luminescence, SAR protocol, water content, archaeology, Late Mesolithic, Norway.

Supervisor(s): Helena Alexanderson and Amber Hood

Subject: Quaternary Geology

Elin Jirdén, Department of Geology, Lund University, Sölvegatan 12, SE-223 62 Lund, Sweden.
E-mail: jirden.elin@gmail.com

Sammanfattning

ELIN JIRDÉN

Jirdén, E., 2022: OSL datering av den Mesolitiska lokalen Nilsvikdalen 7, Bjorøy, Norge. *Examensarbeten i geologi vid Lunds universitet*, Nr. 633, 34 sid. 45 hp.

Sammanfattning: Luminiscensdatering är en väletablerad dateringsmetod inom geologisk och arkeologisk forskning. Dock är användandet av luminiscensdatering, mer specifikt optiskt stimulerad luminiscens (OSL), fortfarande underrepresenterat inom norsk arkeologi. Denna studie ämnar utreda lämpligheten av denna dateringsmetod som ett användbart alternativ för utgrävningar av Stenålderslokaler på den norska kusten. Detta genomförs genom att OSL-datera sex prover från tre successiva kulturlager av en boplats (Nilsvikdalen 7) på Bjorøy, sydvästra Norge, vilken tidigare har kol-14-daterats till Senmesolitikum. Från resultaten kan sedan metodens lämplighet utvärderas.

Kulturlagren består alla av varierande grad humus-rik sand med träkol, där OSL proverna togs från in- och utsida av vad som tolkats som en hydda. OSL-datering av kvarts genomfördes för alla sex prover genom användande av SAR protokollet och gav framgångsrika resultat. Proverna uppvisade en stark kvartssignal med utmärkta egenskaper. Vattenhaltsmätningarna resulterade i de största osäkerheterna för bestämning av bakgrundsstrålningen, men bestämdes efter noggrann avvägning till ~ 63 – 114%. Bakgrundsstrålningen bestämdes till ~ 2 – 4 Gy/ka. Olika åldersmodeller applicerades, där medelåldern användes för den slutgiltiga åldersbestämningen. Det understa kulturlagret daterades till Senmesolitikum, med OSL-åldrar av 8.07 ± 0.51 ka och 7.02 ± 0.43 ka inne i hyddan samt 6.60 ± 0.40 ka utanför hyddans gräns. Det mellersta och översta kulturlagren daterades till Senmesolitikum – Tidigneolitikum, där det mellesta lagret gav en ålder på 6.25 ± 0.36 ka och det översta lagret gav åldrarna 5.56 ± 0.32 ka och 6.94 ± 0.36 ka (alla dateringar inne i hyddan). Tre av proverna överlappar åldersmässigt med ^{14}C -åldrarna för respektive lager, medan de andra tre skiljer sig statistiskt (värden utanför ± 2 σ) från ^{14}C-åldrarna. För proverna med statistisk skillnad är OSL åldrarna alla yngre än respektive kol-14-dateringar.

För framtida OSL-dateringar föreslås det att, vid möjlighet, ta ett kontrollprov av recent eller känd ålder från lokalen för att reducera möjliga osäkerheter inom luminiscens-åldersdateringen. Med den lyckade dateringen av boplatsen Nilsvikdalen 7 demonstrerar detta projekt hur OSL-datering kan bidra som ett gott alternativ för framtida dateringar av Stenålderslokaler i den norska skärgården.

Nyckelord: OSL datering, luminiscens, SAR protokoll, vattenhalt, arkeologi, Senmesolitikum, Norge.

Handledare: Helena Alexanderson och Amber Hood

Ämnesinriktning: Kvartärgeologi

Elin Jirdén, Geologiska institutionen, Lunds Universitet, Sölvegatan 12, 223 62 Lund, Sverige.
E-post: jirden.elin@gmail.com

1 Introduction

The use of luminescence dating in both archaeology and geology is well established (Duller 2008a), with several reviews on the development and application of luminescence dating within archaeology now available (Roberts 1997; Feathers 2003; Jacobs & Roberts 2007; Wintle 2008; Roberts et al. 2015). The possibility of dating both burnt artefacts and unheated sediment using luminescence offers an alternative chronometric method for determining the ages of sediment at archaeological sites where other methods might not be suitable, e.g., radiocarbon dating. However, while luminescence is increasingly applied in multi- and interdisciplinary research as a viable dating method, it remains underutilised in Scandinavian archaeology as evidenced by the few publications currently available.

Luminescence dating, and especially OSL dating, offers several advantages compared to other chronological methods and it stands to reason that OSL should be even more frequently applied in future archaeological investigations. Such advantages include, but are not limited to, determining the timings of site occupational history and depositional rates, or simply having an alternative method to rely on other than radiocarbon dating if the site materials should not prove suitable for such dating (Rittenour 2008). OSL dating is in addition able to address problems related to post-depositional sediment mixing, as well as being able to cover a broader age range than radiocarbon dating (Jacobs & Roberts 2007). Specifically, where the limit for radiocarbon dating extends to approximately the last 40 000 years (Rittenour 2008), luminescence dating provides dates from Palaeolithic sites up to 300 000 years (Bateman 2019).

An opportunity to test the use of luminescence dating in an archaeological approach came up when six OSL samples from an excavation of a Scandinavian coastal Stone age site became available for analysis. The excavation, done in 2010, was of a site at Bjorøy, southeast of Bergen, Norway. During the excavation, six OSL samples were taken from a stratigraphic profile of what was interpreted as cultural layers from a hut structure. Furthermore, in 2020 the University museum of Bergen compiled a program of past, current and planned archaeological investigations of Stone age archaeology in Vestlandet, Norway, see Bergsvik et al. (2020). With both the available luminescence samples from a coastal Stone age site and the ongoing archaeological projects in western Norway, OSL dating of the Bjorøy site would serve to not only yield dates for the occupation but also show whether this is a suitable geochronological method for similar sites in the area, seeing as luminescence dating qualities (and thus suitability for successful dating) varies across Scandinavia depending on the geological history (Alexanderson 2022).

1.1 Research questions and purpose of study

The aims of this project are to increase the knowledge and understanding of the Nilsvikdalen site 7 (onwards referred to as Nilsvikdalen 7) at Bjorøy by use of optically stimulated luminescence dating, and to evaluate the potential contribution of luminescence dating to similar geoarchaeological settings. To accomplish this, the project specifically aims to:

1. OSL date six sediment samples from the site and assess what periods they represent,
2. Address how the OSL dates compare to existing radiocarbon dates and the site stratigraphy,
3. Evaluate how luminescence dating is applied today in geoarchaeological settings in similar Scandinavian archaeological sites and discuss the possibilities for future OSL research in the field.

The two first aims specifically address the Nilsvikdalen 7 site, and subsequent results from this case study should be able to provide for the discussion of the third aim; whether the use of OSL dating is beneficial in similar Scandinavian archaeological sites or not.

2 Archaeological applications of OSL

To begin with, this section will address the applications of OSL within archaeology, both generally and specifically for Scandinavian research. Specifically, how it is implemented in Norwegian research today is of interest for the later discussion of whether OSL should be implemented more in future archaeological research.

The application of luminescence dating, both thermoluminescence (TL) and optically stimulated luminescence (OSL), to archaeology is as mentioned widely established; see, for example the multitude of research references in Roberts (1997); Feathers (2003); Jacobs & Roberts (2007); Rittenour (2008); Wintle (2008) and Roberts et al. (2015). Dating has been done on a wide range of contexts, for example, on aeolian sands and occupation debris from settlement sites in South Africa (Feathers & Bush 2000; Chazan et al. 2013) or aeolian sands from Neolithic-Bronze Age coastal sites in Scotland (Sommerville et al. 2007), on mortar to determine construction and building phases in the Saint Seurin Basilica in France (Urbanová et al. 2018), on a tomb, stone walls and ceramics from a Late Helladic site in Greece (Liritzis et al. 2019), of field boundary banks in Cornwall to determine the construction and eventual modifications of them (Vervust et al. 2020) or on deposits from an agricultural infield connected to a settlement mound in Shetland (Burbidge et al. 2001). What links all these sites and makes them suitable for luminescence dating is their containing sediments or objects with minerogenic material suitable for luminescence research. As quartz and feldspar – the two main minerals suited to luminescence dating – are abundant across the earth and present at almost all archaeological sites, this makes luminescence dating applicable to most archaeological questions. Yet, as discussed by Bateman (2019), in comparison to radiocarbon dating, luminescence dating is underrepresented. This is also the case for luminescence dating of archaeological sites in Norway, such as Nilsvikdalen 7.

There is also a multitude of luminescence studies published from Norway, however, these are pri-

marily geological studies; archaeological application of luminescence dating in Norway are extremely limited. To exemplify, dating has been done on glaciofluvial and fluvial deposits (Bøe et al. 2007; Johnsen et al. 2012), glacial sediments (Anjar et al. 2018), aeolian dune field deposits (Alexanderson & Henriksen 2015), Holocene flood deposits (McEwen & Matthews 2013) and on Holocene raised beach deposits (Fuchs et al. 2012).

With this being said, there are some applications of luminescence dating more broadly across Scandinavian archaeology and multidisciplinary research (i.e., research focusing on OSL dating landforms or sediment in direct association with archaeological activity). For example, Murray & Clemmensen (2001) dated both coastal dunes and an archaeological site in Thy, Denmark, to date stormy periods 4500 years ago. Another example is how OSL dating of beach ridges has been used to help understand Late Holocene coastline dynamics in Kristiansen et al. (2021), where they used this to understand and correlate the coastal environmental conditions in isostatically-uplifted areas of northern Denmark with prehistoric settlement patterns. There are also studies dating stone structures or heated artefacts, such as Baran et al. (2003) where sediment between a stone wall and a clearance cairn were OSL dated to determine the construction age of the site, or in Finland, where a coastal stone age site was dated by Eskola et al. (2003) by using OSL to date sand situated underneath heaps consisting of heated stones and TL to date the heated stones. Similarly, Vafiadou et al. (2007) used OSL to date soils from a floor-layer and rock samples from a burial mound in Scania. Post-Infrared Infrared stimulated luminescence (Post-IR IRSL) dating, in addition to OSL, has also been carried out on pre-roman Iron- and Viking Age heated stones and ceramics in al Khasawneh et al. (2015). Søe et al. (2017) did a multidisciplinary landscape reconstruction in Illerup, Denmark, where OSL was incorporated to understand the choice of location for an Iron Age ritual deposition. Nielsen & Dalsgaard (2017) performed a similarly multidisciplinary study, here on Celtic fields in Jutland, Denmark; Using methods including particle size analysis, geochemistry, radiocarbon dating, OSL, and pollen- and macrofossil analysis, they dated the field banks to the late Bronze Age – early Iron Age. Both Søe et al. (2017) and Nielsen & Dalsgaard (2017) are especially important studies, as they present clear examples of engaging in multidisciplinary research of archaeological sites, such as has occurred at Nilsvikdalen, to better interpret the archaeology of the site. Thus, while luminescence dating has been underutilized in archaeological investigations in Norway, this illustrates the clear potential for it to be used in archaeological applications in many different settings. There are multiproxy studies published for Norwegian Stone Age dating research, such as seen Bergsvik et al. (2021), and to also incorporate OSL dating as an independent age control or for age determinations where no other methods are suitable in the region pose a great possibility.

3 Regional background

3.1 Geological setting

Bjorøy is situated in the archipelago approximately 10 km outside of Bergen, western Norway (Fig. 1). The dominating bedrock on Bjorøy is a granitic gneiss belonging to the Øygarden Complex (Fossen & Ragnhildstveit 2008), which is a part of the larger Bergen Arcs System and was metamorphosed during the Caledonian Orogeny (Knudsen & Fossen 2001). The gneisses of the Øygarden Complex are often mylonitic, as well as varying in composition between being granodioritic and granitic (Fossen et al. 1997). A risk for high levels of radon have been reported for Bjorøy as well (Norges Geologiske Undersøkelse n.d.-b).

Most of Bjorøy consist of bare bedrock where only minor Quaternary deposits can be found (Fig. 1), namely peat and till (Norges Geologiske Undersøkelse n.d.-a). From the deglaciation reconstruction by Stroeven et al. (2016), Bjorøy and the surrounding Bergen area was fully deglaciated during the Allerød after a slow deglaciation in the coastal areas with some areas experiencing readvances during the Younger Dryas. Entering the Early Postglacial, the colder arctic climate was replaced by a warmer climate; with an initial habitation of subarctic-boreal vegetation (Bjerck 2008). At 9000-8500 yr BP the Tapes transgression begun and caused a sea level rise which culminated at 6000 yr BP, where traces of both this event as well as from a tsunami (the Storegga tsunami) is recorded at multiple sites in western Norway (Bondevik et al. 1998).

3.2 Archaeological setting

As there exist some variation in what calibrated ages are assigned for the archaeological periods in published papers, this study will follow the ages presented in Bergsvik et al. (2020) (Table 1).

Norway was colonised rapidly during the beginning of the Early Mesolithic (Bjerck 2008), with a clear trend of the sites being located coastally during the Early Mesolithic to Middle Neolithic (Bergsvik et al. 2020). In general, these Stone Age settlements appear as open air sites rather than other types of settlements (Hjelle et al. 2006; Bjerck 2008).

The population during the Early Mesolithic focused largely on marine resources and rather than staying fully sedentary they moved around more in smaller groups (Bjerck 2008; Bergsvik et al. 2020). Evidence of more sedentary settlements (although remaining mobile) among the hunter-fisher communities is recorded at the Fosnstraumen settlement, north of Bergen, during the following Late Mesolithic to the Middle Neolithic (Bergsvik 2001). This follows the general trend of increased permanent settlements but also a wider regional differentiation between sites seen in the Middle and Late Mesolithic (Bjerck 2008). When entering the Middle to Late Mesolithic periods the archaeological site finds also start to vary more, from the Early Mesolithic tent structures and fire pits there is now also sites with stone settings and cooking pits to mention some (Bergsvik et al. 2020). However, here the authors note how this just could be a case of more variation present due to having excavated more sites from these periods (Bergsvik et al. 2020). It

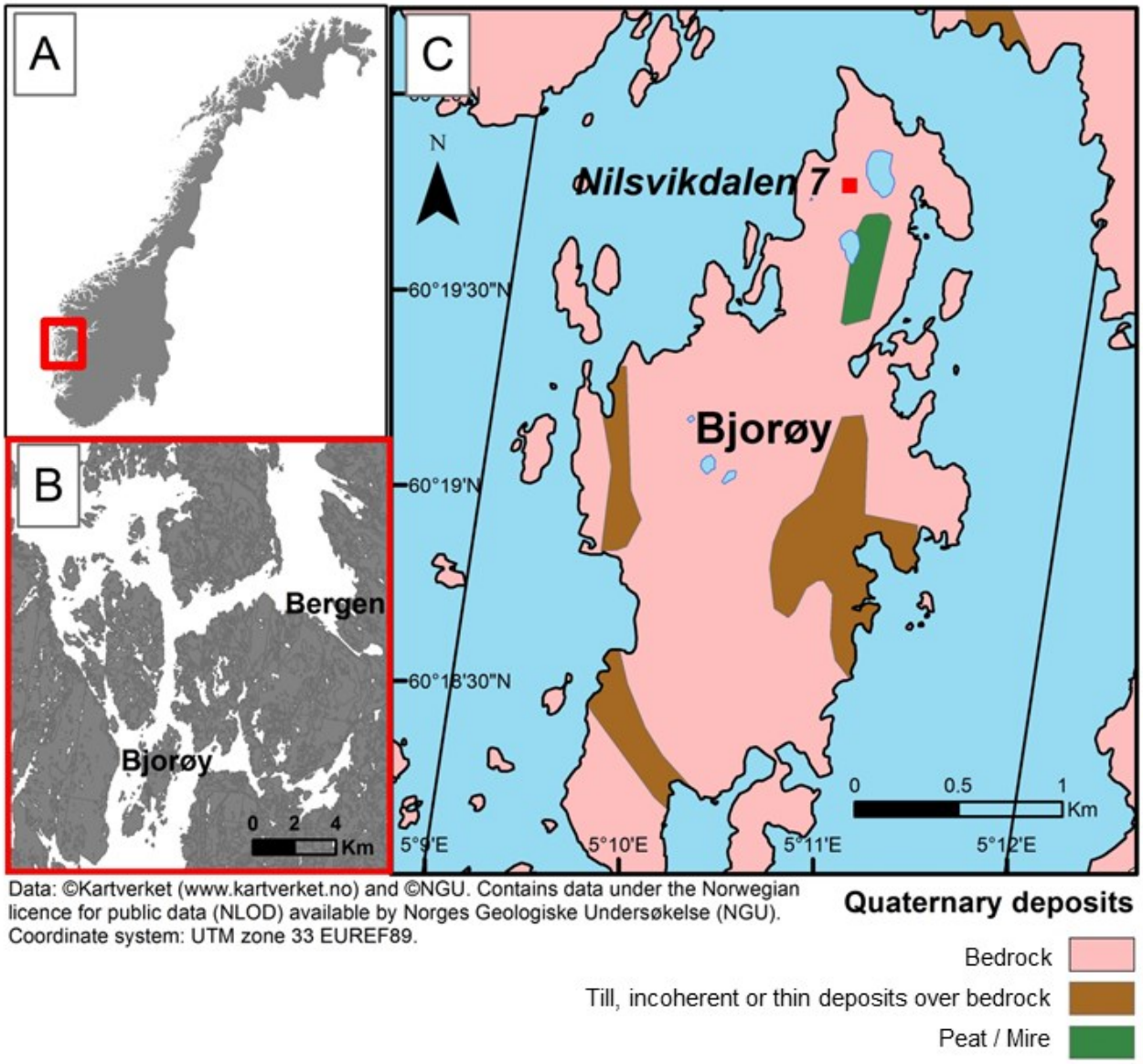

Fig. 1. Location of the study site. Map created in ArcMap 10.5.1. **A.** The regional location of Vestlandet and the site in Norway. **B.** Local map over parts of Vestlandet archipelago, with Bjorøys location in relation to Bergen. **C.** Bjorøy and its Quaternary deposits, with the Nilsvikdalen 7 site marked in red. Note how resolution of the Quaternary deposits are not mapped in as great detail as desired here, and Nilsvikdalen is in fact also covered by thin layers of peat/mire deposits.

should also be mentioned how, due to the rising sea level during the Holocene transgression, the majority of the Middle Mesolithic coastal sites have disappeared (Bjerck 2008). It is first in the Late Neolithic there is evidence for agriculture (Halvorsen & Hjelle 2017), although it is pointed out how some smaller scale animal husbandry and cultivation was present before the Late Neolithic agricultural introduction (Hjelle et al. 2006).

3.3 Previous work at the Nilsvikdalen 7 site

There have been several previous excavations of Mesolithic and Neolithic sites on Bjorøy: during the 1990s a total of 15 sites were excavated in the area (Bergsvik et al. 2020). The Nilsvikdalen 7 site is situated on the northern part of Bjorøy, approximately 10 km southwest of Bergen. The Nilsvikdalen area was previously excavated and documented by Kristoffersen (1995). The area was excavated again in 2010 by Åstveit et al. in prep (2022) where, underneath the peat deposits covering the site, a hut feature was discovered. The structure and the lithic inventory were interpreted to be Late Mesolithic, and in close proximity to it a Neolithic site was discovered. During the period of Mesolithic occupation, the site was more closely situated and connected to the sea due to higher waterline conditions and today the Mesolithic cultural layers are located on an elevated area (Åstveit et al. in prep 2022). Similar locations have been documented at multiple archaeological long-term settlements in the area (Åstveit et al. in prep 2022), indicating comparative habitation and deposition events across the region.

Table 1. The archaeological ages of interest for this study. The archaeological periods and their corresponding calendar years are all from Bergsvik et al. (2020) and are here in addition converted to cal. BP years as well as ka BP.

Archaeological period		Calendar years (cal. BC)	Age (cal. yr BP)	Age (ka BP)
Mesolithic	Early	9500–8000	11450–9950	11.5–10.0
	Middle	8000–6500	9950–8450	10.0–8.5
	Late	6500–4000	8450–5950	8.5–6.0
Neolithic	Early	4000–3300	5950–5250	6.0–5.3
	Middle A	3300–2600	5250–4550	5.3–4.6
	Middle B	2600–2350	4550–4300	4.6–4.3
	Late	2350–1800	4300–3750	4.3–3.8

4 Luminescence dating background

Luminescence dating is an umbrella term for a wide variety of dating methods (e.g., thermoluminescence, optically stimulated luminescence, infrared stimulated luminescence or other variations) relying on the emission of a luminescence signal. What all the methods have in common is how a luminescence signal is built up over a period of time in mineral grains, usually of quartz and feldspar. More specific, electrons are excited from their original places in the valence energy band to the conduction energy band owing to exposure to radiation; subsequently when the electrons then exit the higher energy states in the conduction band, some become trapped and stored in electron traps which are defects in the mineral's crystal lattice (Preusser et al. 2008; Bateman 2019) (Fig. 2). The dose calculated from the magnitude of this built-up signal is what allows for an age determination when divided with the dose rate.

The last exposure to light or heat will serve as a reset (zeroing) event for the luminescence signal in the sediments from which the signal will start to rebuild again after deposition (Aitken 1998), optically stimulated luminescence (OSL) thus allows determination of the last time the sediments were exposed to light or heat (Duller 2008a; Preusser et al. 2008). This possibility to date not only burnt or heated artefacts, but sediments as well from an excavation site is why OSL dating is such a crucial geoarchaeological dating method. Another aspect of its importance, as already mentioned, is how it can date much older material as compared to radiocarbon dating and is of course not reliant upon the preservation of organic material (Jacobs & Roberts 2007; Rittenour 2008; Bateman 2019).

As for the different luminescence techniques available there are some significant differences. Between thermoluminescence (TL) and OSL there are several key points. Briefly summarized, TL relies on heat as the energy necessary to empty the electron traps, whilst OSL utilizes the energy from light (Bateman 2019). The OSL technique was pioneered in a study by Huntley et al. (1985) where they examined sediments from different geological settings to determine their ages by OSL, and compared the past radiation dose acquired for sediments where they already had the known ages and different known radiation dose measurements. After this initial application, the term has come to include several different methods relying on stimulation by light; such as Infrared stimulated luminescence (IRSL) or linearly modulated OSL (LM-OSL) (Preusser et al. 2008) and later improvements in both technology and knowledge has been accomplished (Duller 2004).

Another importance of distinguishing between the different luminescence techniques is how they display different advantages. There exist several technical advantages of OSL compared to TL. One of them is how OSL samples rely on shallower electron traps than TL, which results in the samples being more easily reset and thus improves the age accuracy and precision (Duller 2004; Hood & Schwenninger 2016). Furthermore, OSL dating can use both quartz and feldspar grains as dosimeters, however, quartz is preferrable since it does not display anomalous fading like feldspar does (Duller 2008a; Preusser et al. 2008).

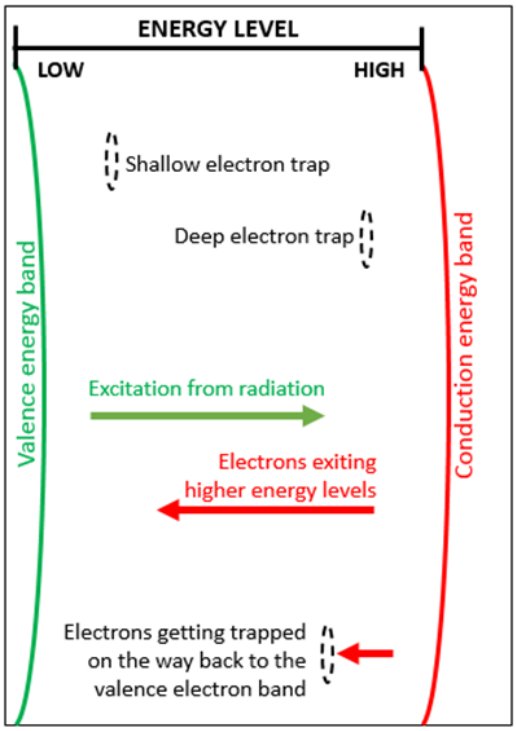

Fig. 2. The procedure for electrons getting excited, leaving the valence energy band, entering the conduction energy band and some getting trapped on the way back. Modified from Preusser et al. (2008).

As discussed in Hood & Schwenninger (2016) using quartz also has the advantage of producing a less complicated luminescence signal than signals produced from TL measurements. To summarize, what all the advantages of OSL presented above display is how the precision and accuracy of the age determinations are improved. Coupled with this, OSL samples require smaller sample sizes, down to single grains if needed (Hood & Schwenninger 2016). This allows for sampling where material might be scarce as well as a possibility of performing more measurements on the sampled material even though it might be limited. Additionally, if single grain OSL dating is used this provides possibilities of determining post-depositional mixing to potentially achieve a more secure age determination (Jacobs & Roberts 2007), where the post-depositional mixing also might be of interest for the archaeological development of the site.

4.1 OSL age calculation factors

When determining the luminescence age there are several factors to consider. Determination of the paleodose, i.e., the equivalent dose (D_e), and the dose-rate ($\dot{D}$) is essential, and within these there are other factors to consider as well. This section will briefly outline the most important factors and problems to investigate to achieve a reliable age determination.

The basic calculation of the luminescence age is shown in equation (1). The equivalent dose (D_e) represents the total absorbed dose calculated by laboratory induced luminescence and the dose rate ($\dot{D}$) is the rate at which the sample receives a dose from its depositional environment (Duller 2008a).

$$Luminescence\ age\ (ka) = \frac{Equivalent\ dose\ D_e\ (Gy)}{Dose\ rate\ \dot{D}\ (^{Gy}/_{ka})} \quad (1)$$

The dose rate is dependent on three separate factors: the cosmic, internal and external radiation (Preusser et al. 2008), i.e., the $\dot{D}_{cos}$, $\dot{D}_{int}$ and $\dot{D}_{ext}$ as seen in equation (2). $\dot{D}_{cos}$ is a result of protons and alpha particles entering the atmosphere and in colliding with each other creating radioactive decay and $\dot{D}_{ext}$ is the radiation received from the surrounding environment through the decay chains of ^{235}U, ^{238}U, ^{232}Th or ^{40}K (Bateman 2019). Regarding the $\dot{D}_{int}$, this is an effect of the possible presence of radioactive elements residing inside the mineral crystal lattice (Preusser et al. 2008), therefore only being present in some cases. All three factors will contribute to the total amount of received dose and will vary between different sites and years. What is important to note is also how the different types of radiation; alpha (α), beta (β) and gamma (γ), effect the grains receiving the radiation differently. Gamma radiation reaches around 30 – 40 cm into the sediment from all directions of the source, beta radiation 1 – 3 mm and alpha radiation only around 20 μm (Bateman 2019). The short distance the alpha radiation reaches is why the alpha contribution is etched away during chemical preparation of a sample. Thus, only beta and gamma radiation need consideration together with the sampling depths. Regarding the external dose rate, the moisture content must be considered since this affects the absorption of the received external radiation, with the water in the sediments effectively shielding the sediments from absorbing a stronger external dose than if the sediments were dry (Preusser et al. 2008). The increased percentage of water content is estimated to reflect the same percentage of increased luminescence age (Duller 2008a). Underestimating the water content might lead to an age determination that might be younger than the actual age, and since water content can vary over the burial time (Bateman 2019) it can be hard to determine the correct water content history.

$$Dose\ rate\ (\dot{D}) = \dot{D}_{ext} + \dot{D}_{int} + \dot{D}_{cos} \quad (2)$$

It is not only the moisture content history, radiation history and sampling depths that must be considered in determining the different factors of the luminescence age. The depositional environment matters when evaluating the D_e: as Duller (2008b) points out some depositional environments present settings where grains will exhibit different D_e values upon their final deposition due to an uneven light exposure. Cases of uneven or incomplete bleaching is also problematic for deducing a luminescence age, and the possibilities for this and other sources of error must be considered in evaluating the validity of the D_e measurements and received ages. There are also some general limits to luminescence dating in that there will be a limited number of traps for the electrons, i.e., a saturation dose, which limits the age determination to a certain maximum age (Preusser et al. 2008; Bateman 2019).

4.2 The Single Aliquot Regenerative-dose protocol

In determining the OSL equivalent dose there are different methods available for choosing the sample aliquots: both Multiple Aliquot and Single Aliquot methods. The former is now used for measuring the equivalent dose in cases of both buried sediments and heated artefacts (Murray & Wintle 2000; Wintle & Murray 2006). The single aliquot method provides a more certain age determination with better accuracy since it can detect partial bleaching more easily (Duller 2008b). Recent developments have also resulted in the ability to analyse single grains, for examples see summary in Roberts et al. (2015). Within the single aliquot methods the single aliquot regenerative-dose (SAR) protocol (Murray & Wintle 2000; Murray & Wintle 2003) has been developed. As discussed in Hood & Schwenninger (2016) the SAR protocol presents improvements in age determination certainty, if compared to TL, in reducing the percentage of D_e measurement error since it utilizes interpolation of the measurement data rather than extrapolation.

The SAR protocol relies on the same aliquot for another round of OSL measurements after the initial measurements have reset the OSL signal and how sensitivity is corrected between measurements (Murray & Wintle 2000). The procedure is illustrated below (Fig. 3), where a typical SAR protocol sequence is illustrated with a given dose, preheat, OSL stimulation, given test dose, cut-heat and lastly OSL stimulated. This process is repeated with several regenerative doses, where one of them is set at 0 Gy and the last regenerative dose will be the same as the first regenerated as a control (Murray & Wintle 2000).

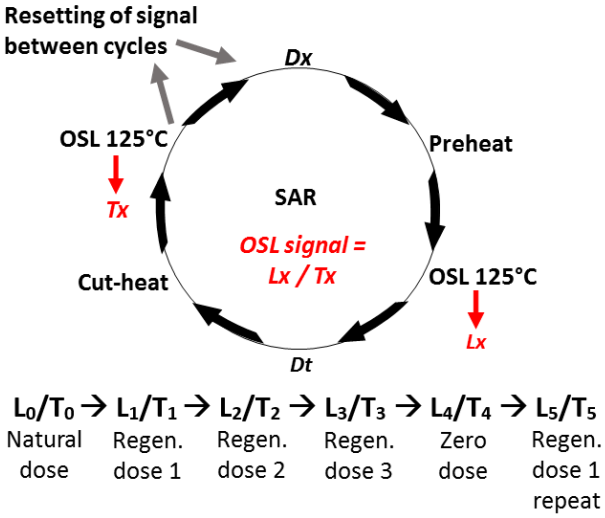

Fig. 3. The SAR protocol procedure modelled after Murray & Wintle (2000). Starting with the given dose (D_x), which varies between different cycles of the SAR protocol, the sample is afterwards preheated and thereafter optically stimulated at 125°C for a predetermined time. This generates the value for L_x. The same procedure is performed afterwards with a test dose (D_t), which generates T_x. The OSL signal is derived from L_x divided by T_x, which is done in cycles of measuring the natural signal (no added dose), regenerated signals 1 – 3, a cycle with no dose and lastly, repetition of the first regenerated signal.

The OSL signal itself consists of several different components. These components were termed the fast, medium and slow components (Bailey et al. 1997). In their study, Bailey et al. (1997) showcased that the components display differences in both growth characteristics and at what energy they are thermally active, which ultimately affects the possibility for partial bleaching of the OSL signal. Since the fast component is the part of the OSL signal from quartz that is wanted for analysis (Wintle & Murray 2006), there are measurements for determining how dominant the fast signal is in the sample as displayed in Durcan & Duller (2011). This control of the fast component may also provide insight to whether parts of the OSL signal originates from thermally unstable components by comparison of the fast ratio between the natural and regenerated signals (Durcan & Duller 2011). The resulting signals can be compiled in a decay curve and a growth curve (Fig. 4) where equivalent dose can be determined from.

4.3 Quality tests to assure correct age determinations

There are several tests to determine the quality and suitability of the quartz and feldspar grains, as well as determination of settings for the SAR sequence. First, to determine what light source to use, depending on feldspar contamination of the sample, an IR test is performed by comparing of one of the regular regenerated doses with the same dose following IR stimulation (Bateman 2019). Secondly, a dose recovery test is done on a fully bleached sample with a known given dose, where the measured D_e is compared to the known laboratory generated dose (Murray & Wintle 2003), indicating whether the SAR protocol settings can be trusted for the measurements (Duller 2008a). For the dose recovery tests, the DR ratio should be as close to a value of 1 as possible, indicating a full dose recovery. Accepted values are within the range of ± 10% from unity, i.e., 0.9 – 1.1 (Murray & Wintle 2003).

In the SAR measurements, the OSL aliquots must be preheated, to ensure the shallower and less stable electron traps to be fully emptied and not inter-

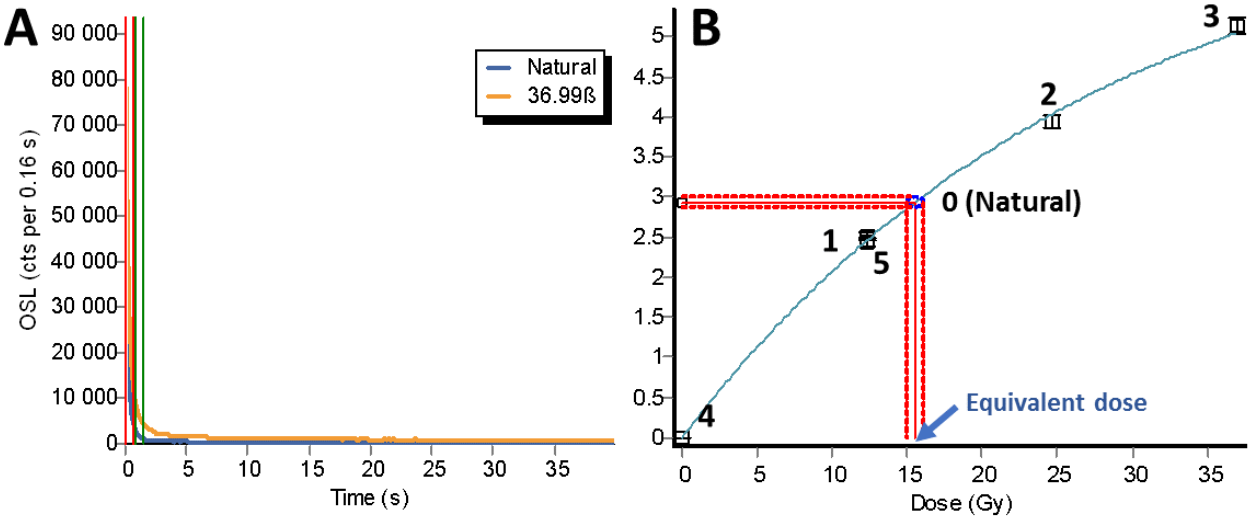

Fig. 4. **A.** The OSL signal is plotted against time in decay curves from an aliquot in sample 21006. The blue curve is the natural signal (before adding a laboratory dose), and the orange curve represents the dose added for the regenerative dose 3. The red lines represent the signal integration limits and the green lines the background integration limits. **B.** The given doses plotted to the OSL signal growth curve from one aliquot in sample 21006. Each dose (natural or regenerative) is plotted in their respective sequence numbers following the SAR protocol sequence as seen in Fig. 3, where 1 = (L_1/T_1) and so forth. Regenerative dose 4 = 0 Gy and regenerative dose 5 is equal to regenerative dose 1. The natural dose gives the equivalent dose (D_e) together with the error margins for the examined aliquot, where from all sample aliquots a mean D_e is derived.

vene in the age determination. The preheat temperature to use is determined in a preheat plateau test, where a range of temperatures are tested to see if they produce acceptable D_e values (Duller 2008a). For the selected range of temperatures, there should be a visible plateau when plotting the D_e against the temperatures. In other words, receiving the same equivalent dose measurement for the range of temperatures that will be selected. For controls within the SAR protocol sequence, there is the recycling ratio test and the recuperation test. The recycling ratio controls the sensitivity correction in SAR by giving the same dose at the start and in the end of the SAR protocol sequence (Roberts et al. 2015), where a value of 0.9 – 1.1 is desired (Murray & Wintle 2000), i.e., within 10% of unity. The recuperation test, which is done by giving the sample the 0 Gy dose, serves as a control of whether the electron traps have been fully emptied or if they have been filled by thermal transfer from the test dose (Murray & Wintle 2000). The recuperation ratio should not exceed 5% of the natural signal (Bateman 2019).

5 Methods

5.1 Field work

Field work was carried out during the 16th to 18th of November 2021, where sites in proximity to Bergen were visited to document the typical characteristics of coastal Stone Age sites in the area and discuss the suitability for luminescence dating at such sites. The Nilsvikdalen site had been destroyed by construction of new infrastructure and no further in situ work or OSL sampling was possible.

5.2 OSL sample characteristics and corresponding radiocarbon dates

The six OSL samples were taken from the site's northern profile (Fig. 5) by Leif Inge Åstveit during the 2010 excavation of Nilsvikdalen 7. Sample one, three and five originate from stratigraphic Layer 9, sample two originates from Layer 8 and samples four and six was taken from Layer 7 (Fig. 6). Layer 9 consist of dark grey to brown/black humus and charcoal enriched sand. Layer 7 is similar, being dark brown to black humus sand with charcoal and layer 8 consist of grey to brown humus sand with some charcoal and clasts (Åstveit et al. in prep 2022). All layers also have high quantities of sand (Halvorsen 2013). As can be seen from the profile's accompanying descriptions, the cultural layers display great similarities and there have been slight uncertainties as to how to divide them (L. I. Åstveit, personal communication, 2022). There is clear evidence of burnt layers and traces of destruction from human activities (Halvorsen 2013), and in the youngest cultural layer (deposited directly before the overlying peat) there have been podzol processes active presenting evidence of drainage in that stratigraphic layer (Åstveit et al. in prep 2022). After sampling, the OSL samples were stored for ~ 10 years before becoming available for analysis for this thesis.

Radiocarbon dating, pollen- and macrofossil analysis were carried out on the site by Halvorsen (2013). The radiocarbon ages (Table 2) relate to the same stratigraphic layers from where the OSL samples were taken. Dating of the bottom, and oldest, layer of the stratigraphic sequence presented an age of 7500 ± 40 BP; the youngest (top) cultural layer dates to 1740 ± 40 BP (Halvorsen 2013; Åstveit et al. in prep 2022).

5.3 OSL lab procedure

All six of the Bjorøy samples were prepared for OSL measurement in darkroom conditions. All samples had been sampled in light proofed tubes with an aluminium foil wrapping. Sample six was sampled in a slightly bigger plastic tube which, in comparison to the others, was the only sample properly sealed with a lid, thus it had more material available for analysis and contained some of the original water content from sampling. The samples were given the codes 21001–21006, following standard lab code assignment at Lund Luminescence Laboratory (LLL). When examining all samples before the chemical preparation, 21001-21005 were all dried out whereas sample 21006 was still moist. It was also noted that 21006 had very dark and fine-grained sediment. There were clasts present in 21002 and 21004, where the latter also notably contained roots.

The samples were treated chemically at first owing to small sample volumes. They were initially treated with 10% HCl for 16.5 hours to remove carbonates and rinsed three times with distilled water. Between each rinse the samples were left for 15 minutes to settle to ensure minimal loss of sediment, since all samples exhibited mostly finer fractions and therefore would take longer time to settle than coarser, heavier grains. There was little to no initial foaming reaction when adding HCl for all samples, indicating a low carbonate content. Organic material was removed by treating the samples with 10% H_2O_2, where slow initial reactions that grew stronger after a few hours

Table. 2. Radiocarbon dates from the stratigraphic profile and their corresponding layers as seen in Fig. 5, dates from Åstveit et al. in prep (2022).

Stratigraphic layer	Sample code	Radiocarbon age (BP)	Calendar age (calibrated)
3	VP 112	1740 ± 40	AD 220–400
6	VP 113	5850 ± 40	BC 4800–4610
7	VP 114	6120 ± 40	BC 5210–4940
8	VP 115	6590 ± 40	BC 5620–5480
9	VP 116	7500 ± 50	BC 6450–6240
9	VP 121	5230 ± 40	BC 4220–3960

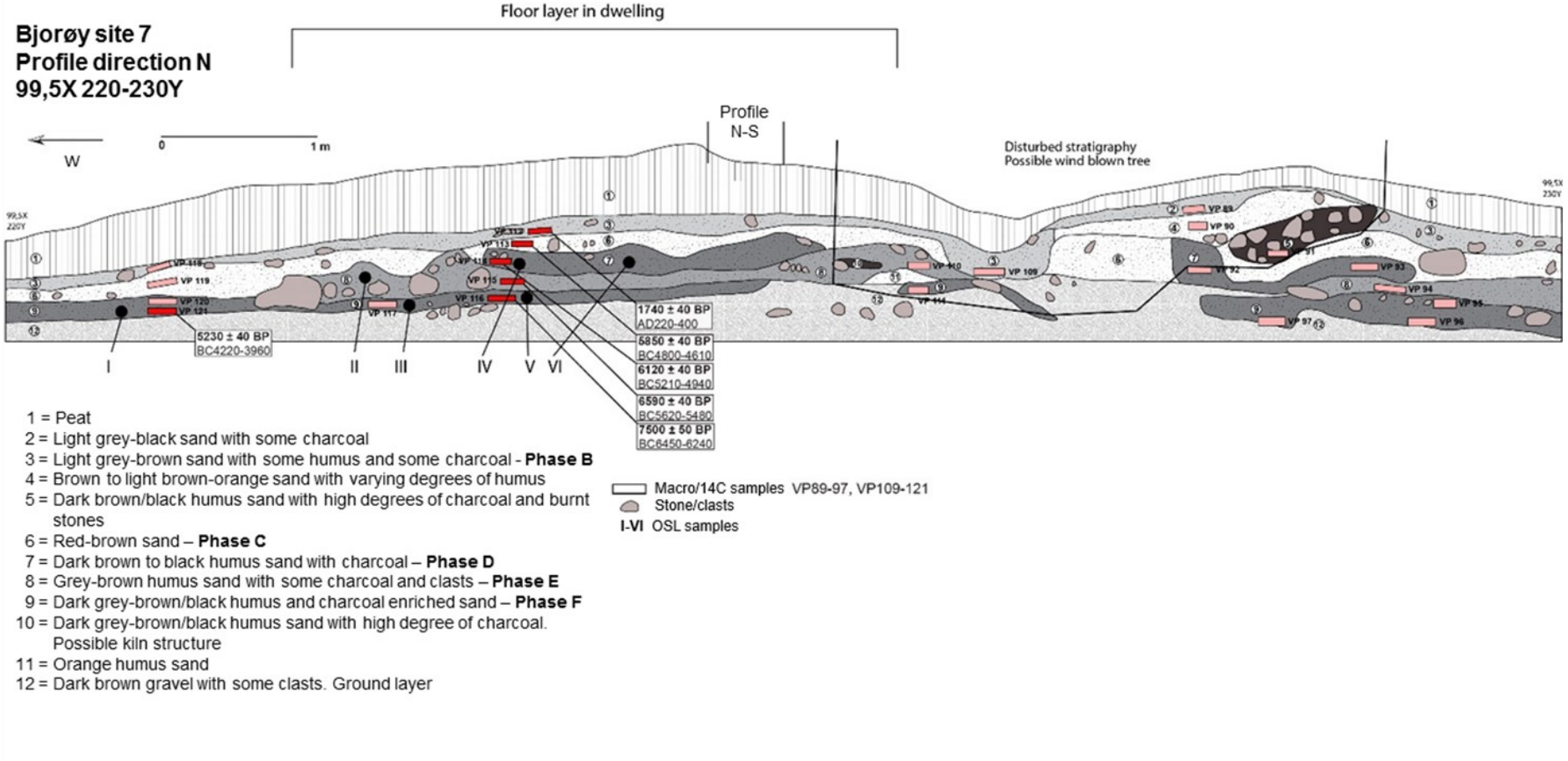

Fig. 5. The site profile from Åstveit et al. in prep (2022), edited by the Author. Marked are the investigated area of the floor layer, the disturbed stratigraphy from a possible windblown tree as well as where in the stratigraphic units the samples for OSL dating, radiocarbon dating, pollen- and macrofossil dating were taken.

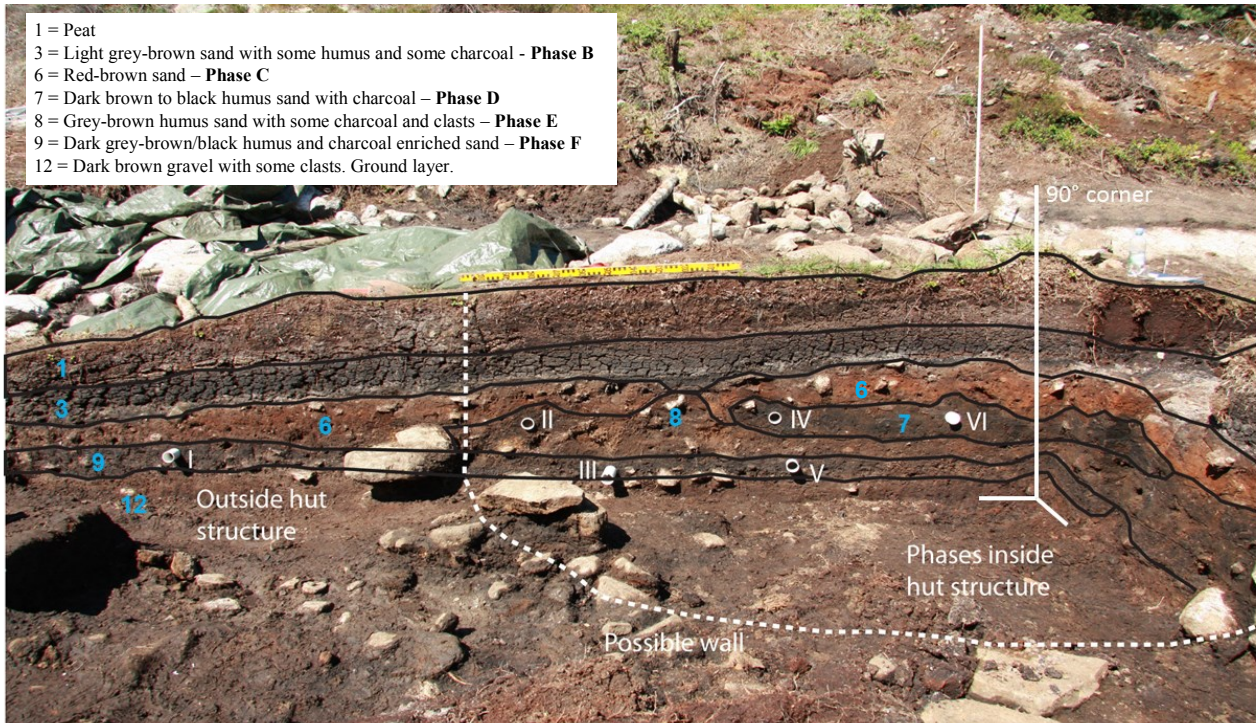

Fig. 6. Picture of the profile stratigraphy with marked borders between the interpreted layers and indications of where the hut structure is situated. Roman numerals represent the OSL samples taken and blue numbers the stratigraphic layers. Picture by Leif Inge Åstveit (University of Bergen), modified by the Author.

were observed. In total, the H_2O_2 was changed and refilled three times before rinsing the samples with distilled water three times. The samples were dried and sieved in fractions of <250 µm and >250 µm before density separation was carried out on the <250 µm fraction for separation of quartz and feldspar grains in the samples. The density of LST Fastfloat (sodiummetatungstate) was 2.62 g/cm^2. Feldspar naturally has a lighter density than this, resulting in it floating on top of the LST Fastfloat. On the other hand, quartz have a higher density and will consequently sink to the bottom of the LST Fastfloat together with other heavier minerals. Samples were left for 24 hours before separating the quartz and feldspar fractions and drying them overnight. Afterwards, the feldspar samples were stored while the quartz samples of <250 µm were etched in HF (40%) to remove any contribution from alpha radiation and other impurities and lastly, to remove any fluorides that might have formed, samples were treated with 10% HCl. The quartz samples were also manually separated from magnetic materials to ensure minimal to no disturbance when measuring the luminescence signal. The samples were lastly sieved again, now into grain size fractions of <63, 63 – 90, 90 – 125, 125 – 180 and 180 – 250 µm.

Sample 21006 was chosen as a representative sample for the quality control tests as well for additional tests of all fractions, mainly based on the large sample volume available and the stratigraphic layer it originates from being situated centrally in the profile within the interpreted hut structure. It also has a sediment composition (dark brown to black humus-rich sand with some charcoal), as seen from the stratigraphic layer Sample 21006 originates from (Fig. 6), that does not differ greatly from the other cultural layers, as seen from the excavation.

Luminescence measurements were carried out with a Risø TL/OSL reader model DA-20 with blue light (470 nm) stimulation, for details on instrumentation see Bøtter-Jensen et al. (2000). The quality tests performed were an IR test, preheat plateau test, dose recovery (DR) test and a bleaching test. 125 – 180 µm was the decided target fraction for the luminescence measurements and except otherwise stated, this is the fraction used. Aliquots of 2 mm were used, where grains per aliquot is estimated to vary between <100 and 100 – 1000 (Fig. 7). The preheat plateau tests and the DR tests were measured in cycles of β irradiation of 9.25, 18.50, 27.74, 0 and 9.25 Gy with a test dose of 1.54 Gy following the SAR protocol procedure.

The IR test was done on 3 aliquots per sample, in fraction 90 – 180 µm. All tests exhibited good results, (Appendix Table A1), with percentages of the mean natural and laboratory IR/B ratio <10% in all cases, where only 21006 exhibited slightly higher percentages (a mean value of 6%). This allowed for blue OSL light to be used for all samples, owing to the IR/B ratio indicating little to no feldspar contamination and thus only needing to use the wavelengths applicable for quartz, i.e., blue light (Bateman 2019). Two preheat plateau tests were measured, one for temperatures 180 – 260°C and the other for 160 – 280°C (20°C difference between each temperature measured in both cases). From the combined test results (Fig. 8), a plateau can be seen around 180 – 240°C. In combination with the recycling values being closer to 1 for the lower temperatures and the dose recovery tests where standard errors were lower for temperatures 160 – 180°C, the preheat temperature was chosen to 180°C and cut-heat to 160°C. For the dose recovery test all samples were bleached in sunlight, where the ble-

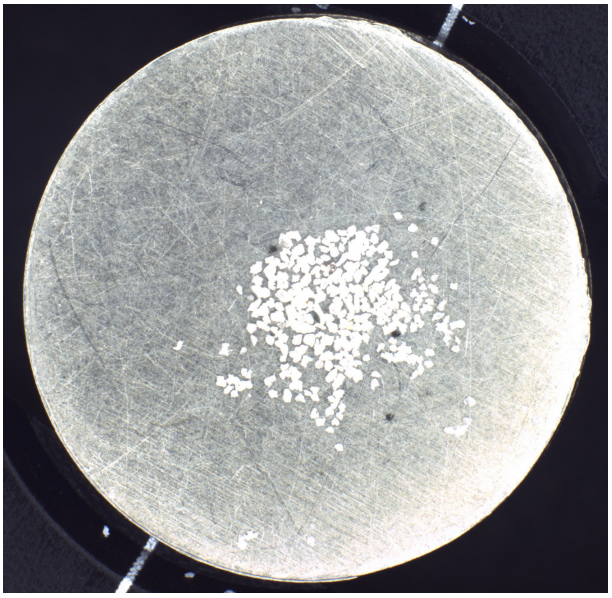

Fig. 7. An aliquot from the IR test; a 2 mm disc with quartz grains mounted on it.

aching time varied between 24 h up to one week. To assure correct bleaching, the aliquots were also bleached in the machine at 90% Blue LED light for 600 s at the beginning of the DR tests. All samples were analysed with 3 aliquots each at the target fraction with an additional DR test containing all fractions of sample 21006 (Appendix Table A2). For all analysed aliquots, the mean DR ratio is 1.02 ± 0.01, displaying a good dose recovery. Only fraction <63 µm (21006) did not pass the criterion of ± 10% from unity, where the mean DR ratio was 1.11 ± 0.02. Considering this fraction had a standard error of ± 0.02 it is on the brink of being acceptable, as well as not being part of the target fraction, and therefore not a problem for continued analysis.

For the equivalent dose measurements, 24 aliquots per sample were analysed. Sample 21003 and

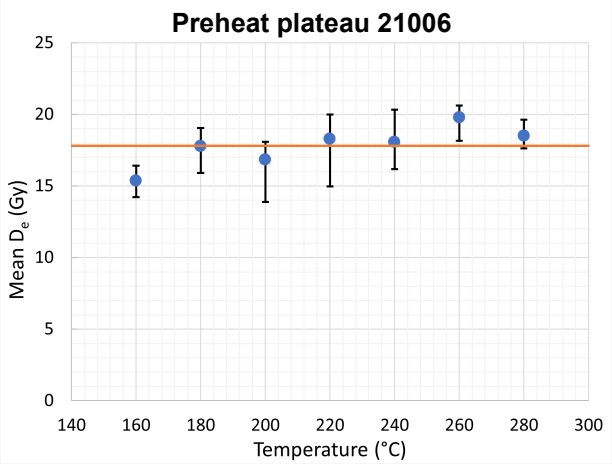

Fig. 8. Preheat plateau for sample 21006. Plotted with the lowest and highest equivalent dose variations recorded per temperature (error bars), the mean equivalent dose per temperature (blue), as well as the overall mean equivalent dose (orange). From this a reasonable preheat plateau can be seen at 180 — 240 °C before there is a slight rise in equivalent dose.

21005 produced D_e values with slightly higher standard deviation error, prompting 24 additional aliquots per sample to be measured. In the D_e measurements β doses of 12.33, 24.66, 36.98, 0 and 12.33 Gy were given to the samples, along with 4.62 Gy as test dose. Preheat was set to 180°C and cut-heat at 160°C. OSL was given at 125°C from blue LED source during 40 seconds at a heating rate of 5°C/s and optical power at 90%. Accepted aliquots had a recycling ratio limit of 10%, max test dose error of 10% and a recuperation of max 5% of the natural signal. Results were analysed in Luminescence Analyst v.4.57 (Duller 2018) with an exponential curve fitting. Calculations were done in MS Excel. Age models following Galbraith et al. (1999) were assigned each sample, following the decision procedure of Bailey & Arnold (2006) and Arnold et al. (2007). The Central Age Model (CAM) and the Minimum Age Model (MAM-3) doses were calculated using R (Burow 2021a; Burow 2021b).

For the dose rate (Ḋ) determination the moisture content, the elemental components (ICP-MS analysis), the burial depth of the sediment and the geographic location and altitude were analysed. Both Ḋ determination and OSL ages are calculated in DRAC, the Dose Rate and Age Calculator (Durcan et al. 2015). Loss on ignition (LOI) was also done by drying the samples at 105°C for 24 h, weighing the sample, heating up at the standard 550°C (Heiri et al. 2001), with a ramping time of 2 hours and 4 hours of 550°C constantly. The samples were weighed again and LOI was calculated (Appendix Table A4). Calculations of the water content were done on both the field sample, i.e., the field water content, as well as on the saturated sample for the saturated water content following Fetter (2014). From the moisture content samples ~ 5 g of each sample was separated and sent off to Actlabs for an Inductively-coupled-plasma mass-spectrometry (ICP-MS) analysis to determine the elemental composition of the samples. The elemental composition, i.e., the U, Th, K and Rb content, of the sediment affects the environmental dose the sample receives since these radioactive isotopes and their daughter isotopes will emit alpha, beta and gamma radiation to their surroundings (Duller 2008a) and is thus vital information for determining a correct dose rate.

6 Results

6.1 Field work

Four coastal Stone Age sites were visited in proximity to Bergen: Nilsvikdalen 7 at Bjorøy, Smivågen at Tyssøy, Kotedalen in Fosnstraumen and Ormhilleren (Fig. 9). These sites can be regarded as common types of coastal sites in different areas of the archipelago during the Stone Age, ranging from larger more permanent settlements to smaller temporarily occupied campsites (B. Nilsson, personal communication, November 2021). For information on Fosnstraumen and Kotedalen see e.g. Bergsvik (2001), however, for Ormhilleren there are no publications available. Given the main objective of investigating the suitability for future OSL dating at typical coastal Stone Age sites, it can be concluded how only some of the archaeological sites visited during the field work would be suited for OSL dating of cultural layers. To exemplify, of the

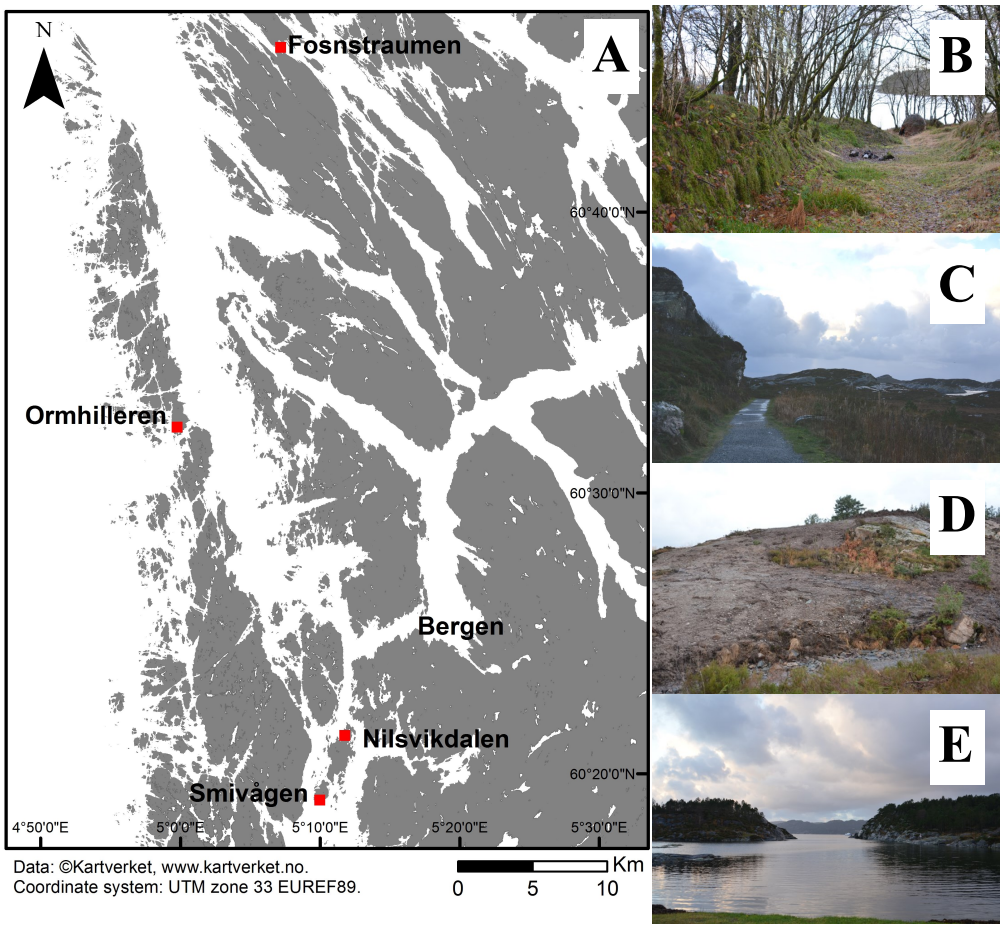

Fig. 9. **A.** Map of the four coastal Stone Age sites visited during the fieldwork; Nilsvikdalen, Smivågen, Fosnstraumen and Ormhilleren. Map created in ArcMap 10.5.1. Field photos from November 2021 of: **B.** Fosnstraumen, **C.** Ormhilleren, **D.** Nilsvikdalen and **E.** Smivågen, Tyssøy.

four sites visited, only Nilsvikdalen and Fosnstraumen would be suitable for OSL dating, whereas the other two sites lacked present cultural layers. However, OSL dating can as previously mentioned be performed on heated artefacts and considering the variation of coastal Stone Age sites and their preservation, the material available for OSL dating and thus the applicability of the method will vary from site to site, see section 7.3 for further elaboration.

6.2 Luminescence measurements

6.2.1 Bleaching test

The bleaching test was done on a slightly cloudy day in central Lund, Sweden. Aliquots for each time interval; 5, 10, 15, 30, 60, 120, 300, 600, 1800 and 3600 seconds, were bleached in natural light conditions. For each time interval, three aliquots were exposed to light, and the average of the three equivalent doses (D_e) were plotted against the logarithmic bleaching time (Fig. 10). The equivalent dose is reduced by ~ 90% during the first 60 seconds, following a D_e signal reduction of ~ 98% after 120 s (Appendix Table A3).

6.2.2 OSL measurements

Results from the ICP-MS analysis, the water content and the resulting dose rates can be seen in Table 3. Dose rates vary between ~ 2 – 4 Gy/ka, with the lowest dose rate at 2.38 ± 0.12 Gy/ka recorded for sample 21006 and the highest at 4.25 ± 0.25 Gy/ka for 21001.

The water content varied between ~ 63 – 114%. Of note is that the water content is similar for the samples within the same stratigraphic layers, where Layer 9 (21003, 21005) display values of 63 – 64% and Layer 7 105 – 114% (21004, 21006). Samples 21001 (Layer 9 outside the hut) and 21002 (Layer 8) both display water contents between 85 – 88%. However, an extensive evaluation was done to determine the correct and final water content to use for the age determination (see discussion section 7.1.2). Therefore, both field and saturated water content were considered independently alongside the resulting environmental dose rates and OSL ages calculated (Table 4).

All samples display relative standard errors of the equivalent dose between 1.33 – 2.57% (Table 5) which is used to determine the precision. This is not to be confused with the precision presented in the radial plots (Fig. 11), which instead is a measurement for the precision of the individual doses in the samples. The samples are also presented in weighted histograms (Fig. 12) as a comparison to the radial plots. Here the samples display narrow and steep curves, where full bleaching of the sample could be seen if the weighted histogram displays a Gaussian distribution (Preusser et al. 2008). Samples 21001, 21004 and 21006 display symmetric dose distributions (Fig. 11 and Fig. 12), while samples 21002, 21003 and 21005 are signifi-

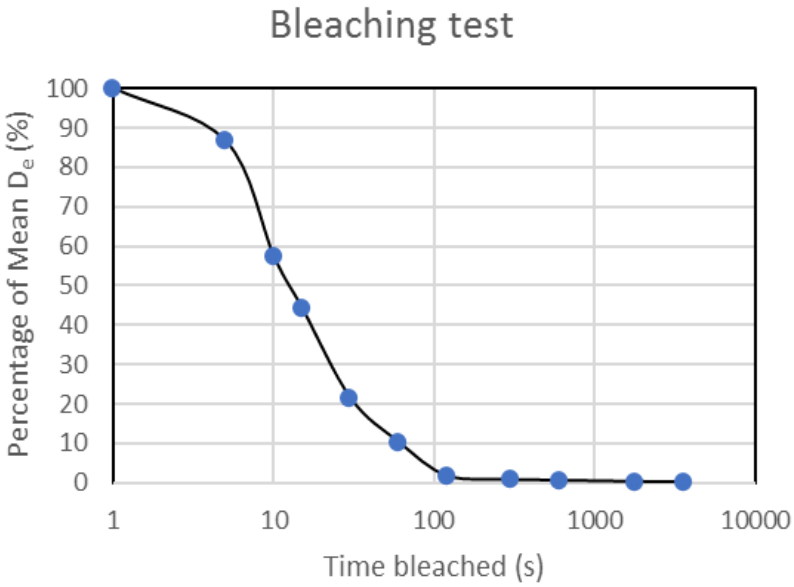

Fig. 10. Bleaching test, with the equivalent doses as percentages of the mean D_e of 21006 left plotted against the time of natural light exposure for the aliquots. After 60 s ~ 90% of the mean D_e is reduced and after 120 s approximately 98% of the signal is reduced, leaving the quartz almost completely zeroed.

cantly skewed (Table 5). There are also slight variations in scatter for 21003 and 21005 which will be discussed later (in section 7.1.1).

All samples have D_e standard errors between 0.22 – 0.73 Gy and a minimum of 24 accepted aliquots, where the highest equivalent dose at 28.04 ± 0.48 Gy was measured for sample 21001 and the lowest at 16.53 ± 0.22 Gy for sample 21006 (Table 5). The overdispersion (OD) values range from ~ 5 – 14%, and the overdispersion calculated from the dose recovery test was 3.8 ± 1.1%.

Ages calculated in DRAC v.1.2 (Durcan et al. 2015) display mean ages between 5.56 ± 0.32 and 8.07 ± 0.51 ka. Additionally, as a control, ages were calculated for all grain size fractions of 21006 (<63, 63 – 90, 90 – 125 and 180 – 250 µm, with 12 aliquots/fraction) where the ages ranged between 7.37 ± 0.41 to 7.08 ± 0.40 ka. Age models applicable for the samples were the Minimum Age Model (MAM) and the Central Age Model (CAM) (Galbraith et al. 1999). The CAM ages yield similar results as the mean ages (albeit slightly younger), between 5.52 ± 0.32 ka and 8.00 ± 0.50 ka, whereas the MAM-3 ages yield ages between 4.71 ± 0.30 ka and 6.78 ± 0.48 ka (Table 5).

For samples 21004 – 21006 the MAM-3 ages were not applicable due to not meeting the statistical controls of the p-value (as derived from the MAM-3 model) where p0>0.05. The ages chosen for site interpretation were the mean ages, which were then plotted against the stratigraphy (Fig. 13). As for the details on the decision made of what age model to use for the final age determination this is elaborated in the discussion (see section 7.1.4).

Table 3. Results of the elemental sample composition from the ICP-MS analysis, water content and the resulting dose rate calculated in DRAC (Durcan et al. 2015). Lower detection limits received from Actlabs.

	U (ppm)	**Th (ppm)**	**K (%)**	**Rb (ppm)**		
Lower detection limit	0.1 ppm	0.1 ppm	0.01 %	2 ppm	**Water content (%)**	
Reported error	10%	10%	5%	10%	10%	**Dose rate (Gy/ka)**
21001	7.3	60	2.3	89	85	4.25±0.25
21002	7.6	39.6	1.9	70	88	3.33±0.18
21003	6.3	27.8	2.5	90	63	3.53±0.20
21004	13.3	31.5	1.9	68	105	3.38±0.18
21005	4.8	26.1	2.9	112	64	3.51±0.20
21006	9.4	22.9	1.4	47	114	2.38±0.12

Table 4. Water content and their resulting environmental dose rates and ages, calculated in DRAC v. 1.2 (Durcan et al. 2015). Water content is recorded with ± 10% error for all measurements.

Sample	Field / Saturated	Water content (%)	Environmental Dose Rate (Gy*ka^{-1})	Age (ka)
21001	F	5	7.87±0.69	3.56±0.32
	S	85	4.25±0.25	6.60±0.40
21002	F	18	5.50±0.43	3.78±0.30
	S	88	3.33±0.18	6.25±0.36
21003	F	7	5.63±0.47	5.07±0.45
	S	63	3.53±0.20	8.07±0.51
21004	F	10	6.56±0.54	2.87±0.25
	S	105	3.38±0.18	5.56±0.32
21005	F	4	5.81±0.50	4.24±0.38
	S	64	3.51±0.20	7.02±0.43
21006-1	F	115	2.36±0.12	7.00±0.36
	S	217	1.63±0.07	10.16±0.45
21006-2	F	114	2.38±0.12	6.94±0.36
	S	127	2.24±0.11	7.37±0.37
21006-3	F	5	5.05±0.43	3.27±0.28
	S	99	2.56±0.13	6.45±0.35

7 Discussion

7.1 Age reliability

OSL dating at the Nilsvikdalen site has, overall, been successful. However, further discussion of these results is necessary to fully understand the data and its nuances. First, the luminescence measurements will be examined, followed by evaluating the different age models, and subsequent interpretation of the site stratigraphy from the OSL age determinations. Lastly, given the results from Nilsvikdalen, the possibilities of future OSL dating at similar sites will be discussed.

7.1.1 Reliability of quality tests and equivalent doses

From the Nilsvikdalen site, the quartz is very suitable for OSL dating; the quality control tests demonstrate bright signals with minimal to no feldspar contamination, a dose recovery within ± 10% of unity, and high precision equivalent dose measurements (~ 1 – 3% error). As a comparison, Alexanderson (2022) reports on quartz quality for luminescence dating in Scandinavia, where samples from good quality quartz also displayed high precision, ~ 2% error. This further confirms the Nilsvikdalen quartz to be of good quality for luminescence dating and indicates how equivalent doses measurements can be trusted to produce reliable ages.

Samples 21003 and 21005 displayed a larger scatter in equivalent doses measurements (Fig. 11 and Fig 12). Because of this, the total number of aliquots examined was increased from the standard 24 to a total of 48, to achieve a more robust assessment of the samples. There will always exist a degree of natural scatter from dose variations between different grains, and smaller aliquots (containing fewer grains) will also have more scatter present due to the lesser number of individual grains to measure compared to larger aliquots (Preusser et al. 2008). The scatter seen from these samples are in other words considered an effect of the larger scatter in dose seen in the first 24 aliquots. With the additional aliquot measurements however, it is possible to achieve a more robust equivalent dose estimate.

Furthermore, as seen in the bleaching test done on Sample 21006 (Fig. 10 and Appendix Table A3), the signal decreases rapidly after 120 s of light stimulation, but, having reached this point decrease in D_e, stabilises as it reaches <2% of the natural signal. In fact, even after 1 minute of exposure on a cloudy day the signal is at 10% of the natural. After one hour of exposure there is still a small residual signal measured, corresponding to only ~ 0.2% of the natural signal and is thus considered effectively zeroed. Godfrey-Smith et al. (1988) studied how long it would require sediments to be exposed to sunlight before their being completely bleached: bleaching in direct sunlight resulted in a decrease to 1% of the original quartz luminescence signal after 10 s. They showed how even on cloudy days the bleaching was complete, as well as how optical dating had a higher bleaching sensitivity than in TL (Godfrey-Smith et al. 1988). Lindvall et al. (2017) performed a similar bleaching test, where they reported bleaching from sunny and cloudy days where the original signals were reduced to <10% after 100 s and a stabilisation of the signal after 1 – 2 minutes. The bleaching signal reported here is not quite as fast

Sample	Accepted aliquots	Suggested Age Model	Skewness (c)	OD (%)	Relative Std. Error D_e (%)	D_e (Gy)	Dose rate (Gy/ka)	Mean age (ka)	CAM age (ka)	MAM-3 age (ka)	p0
21001	24/24	CAM	0.45	6.8±0.3	1.71	28.04±0.48	4.25±0.25	**6.60±0.40**	6.56±0.39	6.12±0.41	0.06
21002	24/24	MAM-3	0.9	6.9±0.3	1.73	20.79±0.36	3.33±0.18	**6.25±0.36**	6.23±0.36	6.14±0.39	0.9
21003	46/48	MAM-3	0.8	13.8±0.3	2.57	28.50±0.73	3.53±0.20	**8.07±0.51**	8.00±0.50	6.78±0.48	0.13
21004	24/24	CAM	0.27	11.3±0.4	2.5	18.79±0.47	3.38±0.18	**5.56±0.32**	5.52±0.32	4.71±0.30	0.02
21005	48/48	MAM-3	0.58	14.4±0.2	2.26	24.62±0.56	3.51±0.20	**7.02±0.43**	6.96±0.42	5.65±0.38	0.01
21006	24/24	CAM	0.03	5.6±0.2	1.33	16.53±0.22	2.38±0.12	**6.94±0.36**	6.92±0.36	6.61±0.38	0.04

Table 5. Equivalent doses with their respective parameters, dose rates and OSL ages. Suggested age models follow the decisional procedure of (Bailey & Arnold 2006). Ages calculated in DRAC v. 1.2 (Durcan et al. 2015). Overdispersion (OD) calculated in Analyst v.4.57 (Duller 2018). Precision is measured from the relative standard error D_e, by dividing the standard error with the equivalent dose for each sample. For the MAM-3 ages, ages were only used if the p-value was p0>0.05. Chosen ages are marked in bold, suggested ages from the age models applicable are marked in blue and red denotes when use of the age model is not advised.

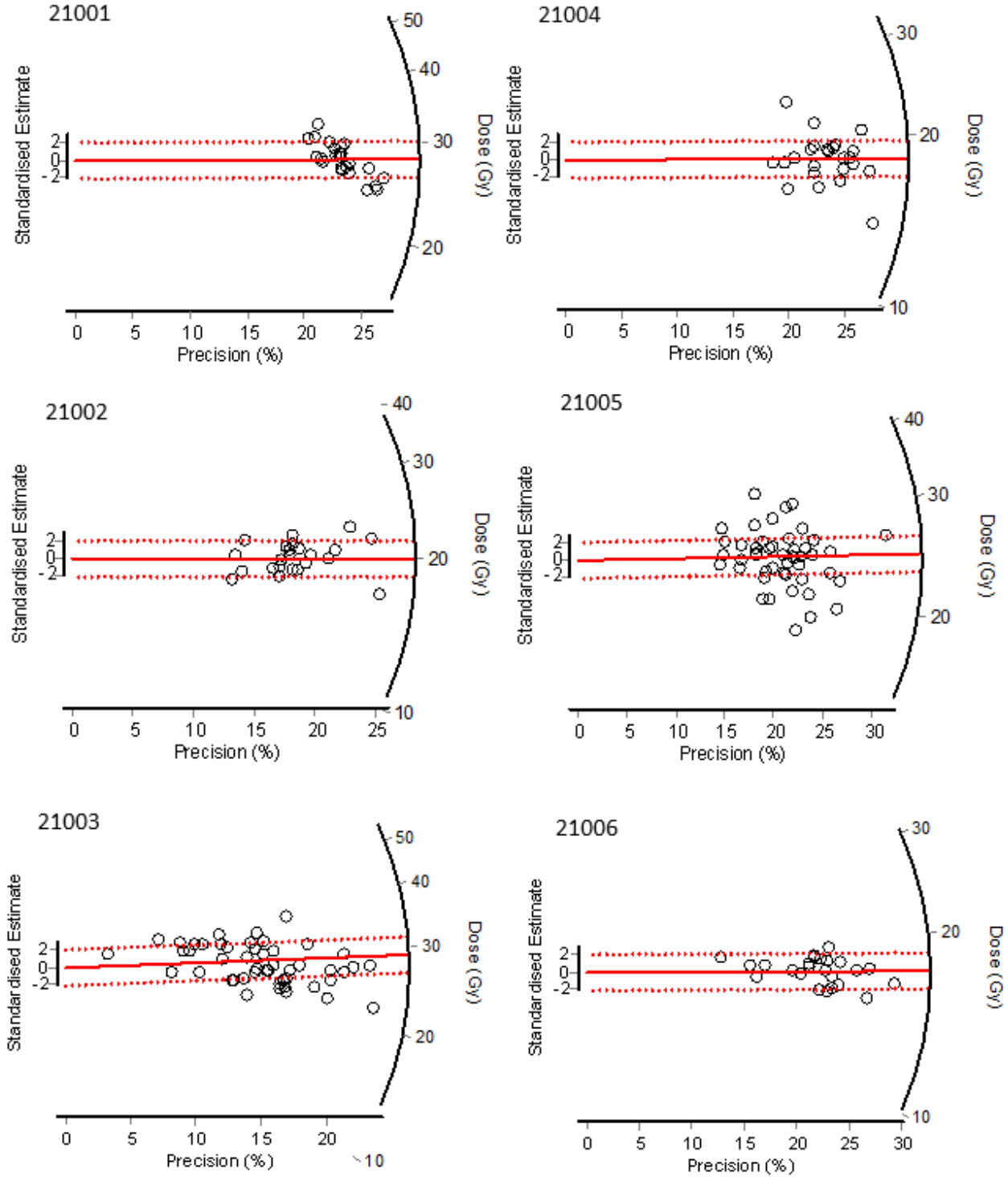

Fig. 11. Radial plots of the equivalent dose results. Plotted with precision (x-axis) and the doses (Gy) for the aliquots (y-axis). The mean dose is marked with a bold red line and the 2 standard deviation estimates in dashed red lines.

as the one reported by Godfrey-Smith et al. (1988), but matches the 10% limit at 100 s and following stabilisation of the signal reported by Lindvall et al. (2017). As seen in all studies, bleaching is successfully completed even in cloudy conditions, and the quartz bleaching rate is quite rapid. Thus, the bleaching test illustrates how the sample material is effectively bleached rapidly under similar conditions as during the experiment. Whether the samples are fully bleached therefore depends on if the conditions during deposition met the criterion of at least 1 – 2 minutes of light exposure. To exemplify, different bleaching outcomes will occur depending on if the sand in the cultural layers were bleached before deposition (e.g., if the cul-

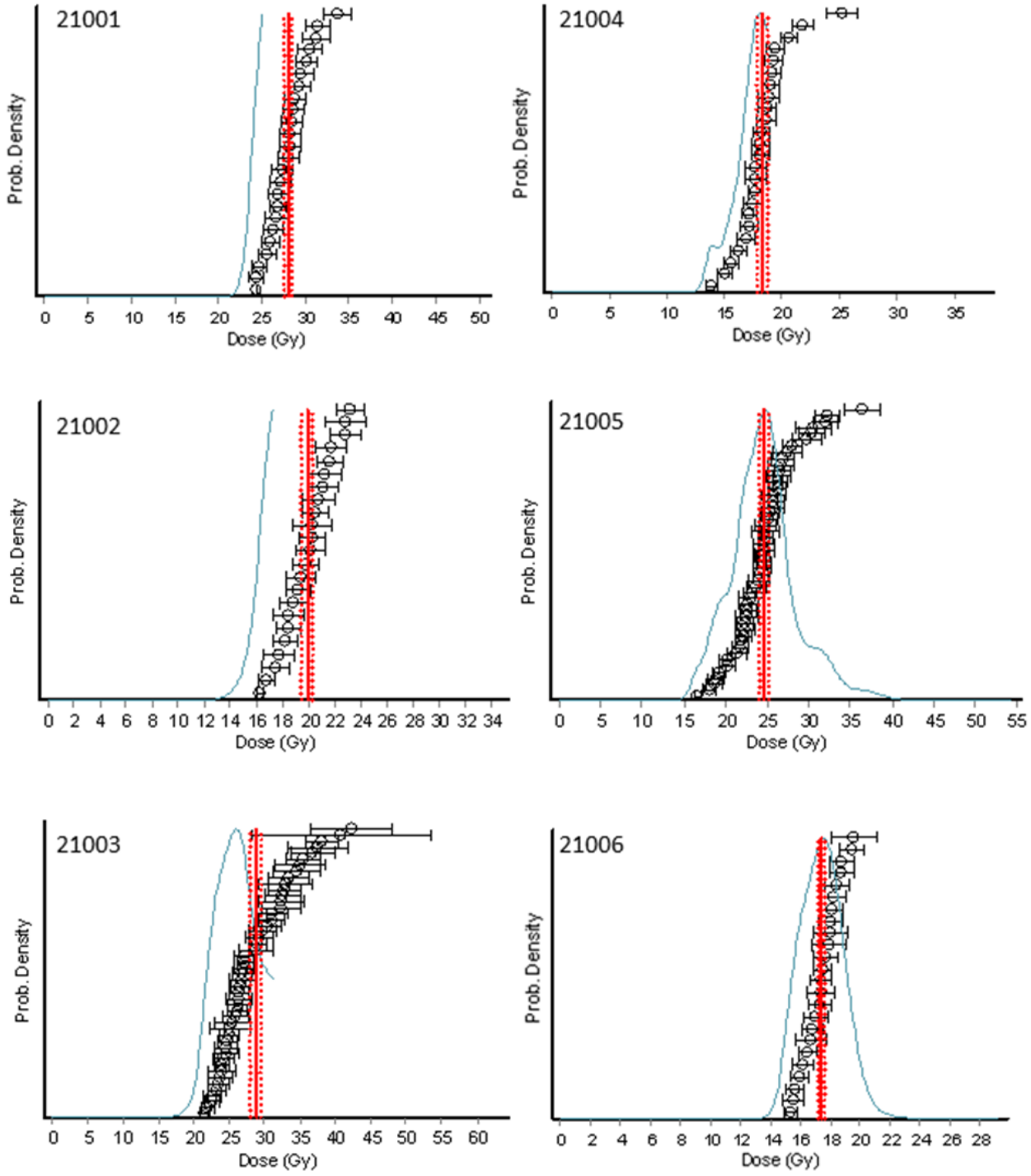

Fig. 12. The equivalent dose results plotted in weighted histograms, where the Gaussian curves show the distribution of the equivalent doses for each sample. The red dashed lines represent the standard deviation, and the bold red line marks the mean dose.

tural layers were specifically constructed by collecting the already fully bleached material and constructing the floor layers) or if bleaching took place after construction of the hut (where the layers were continually accumulated during occupation). In the latter case, consideration of whether the inside of the hut would have seen enough light to fully bleach the new depositional layers would be needed. Regardless of the possibility of incomplete bleaching before layer construction, if the site was seasonally abandoned, bleaching could effectively take place in between occupation. Given the mobility and seasonal settlement of the Mesolithic population (Bjerck 2008), this would be plausible. For the Nilsvikdalen site, it is likely for the settlement to have been occupied in cycles with the site being abandoned in between accumulation of the

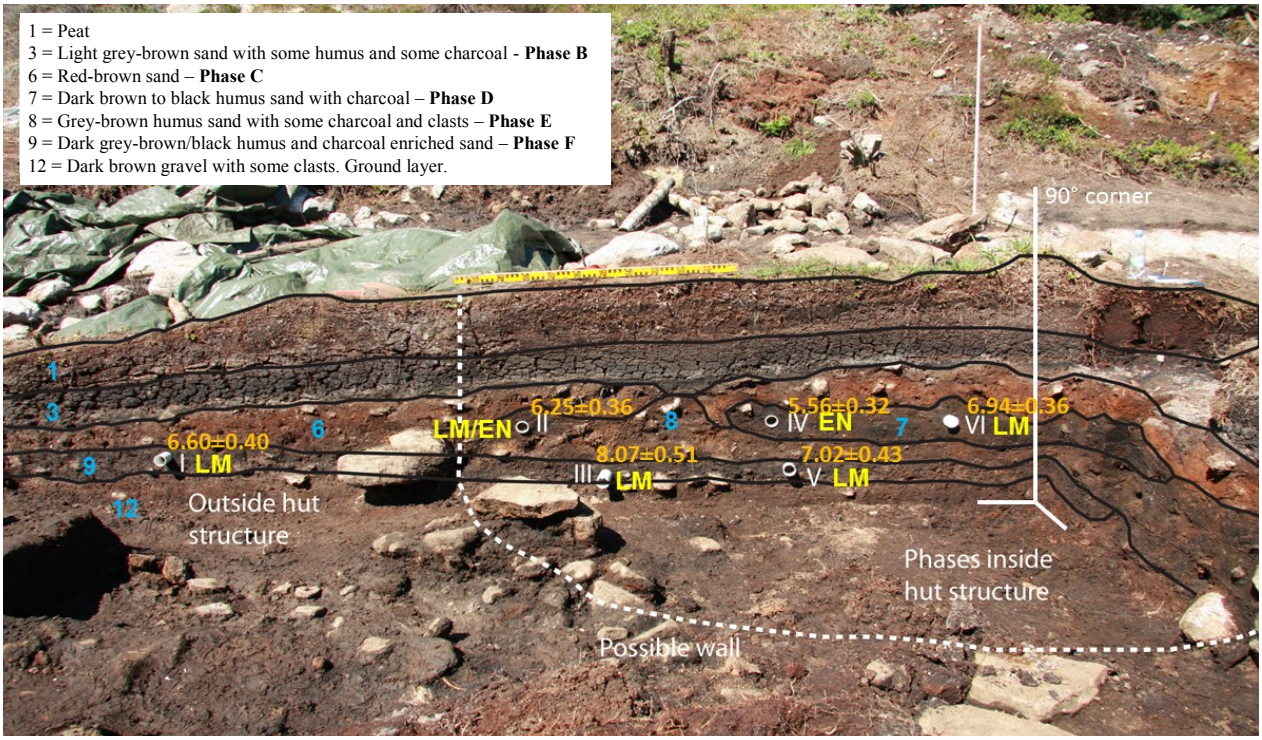

Fig. 13. The stratigraphic layers with the locations for the OSL samples taken and mean ages (ka) plotted in orange. Roman numerals represent the OSL samples (21001 = I, etcetera), the stratigraphic layers in blue numbers and the assigned archaeological periods are seen in yellow. LM: Late Mesolithic and EN: Early Neolithic. Photo: Leif Inge Åstveit, University of Bergen, modified by the Author.

different cultural layers (L. I. Åstveit, personal communication, May 11, 2022). This suggests the bleaching criterion to be met at least in between occupation, however, further investigation into this matter would be of interest.

7.1.2 Dose rate uncertainties – water content influence

Since the quality tests and D_e measurements performed exceptionally well, possible uncertainties for the age reliability mainly depend on the dose rate (Ḋ) determination. In fact, the largest age determination errors are often derived from the Ḋ determination uncertainties (Bateman 2019). Within the Ḋ determination, the determination of the water content is often where the largest variations in age arise (Duller 2008a), particularly for sites such as Nilsvikdalen. This is especially the case where the water content (or other parameters affecting the dose rate) is known to vary over the burial history, creating a dose rate that is time dependent as discussed in Degering & Degering (2020).

There is a large spread in calculated percentages from the field and saturated water content (Table 4). The field water content ranges from 4 – 18% and the saturated water content range from 63 – 105% for samples 21001 – 21005. Sample 21006 stood out, with initial measurements of 115% and 217% for the field and saturated water contents respectively. The saturated percentage is too extreme to be considered reliable and since the field water content is also high in comparison with the other samples, the measurements were repeated. The field water content for 21006-1 and 21006-2 are both taken directly when opening the sealed container, thus these field water contents of 114% and 115% (although still high) are the field water contents with the most accurate representation of the water content present at the site during sampling since the other samples had already dried out during storage. 21006-3 was done as a test on a similarly dried-out sub-sample of Sample 21006. Seeing as this test clearly matches the values received for the other dried out samples, it can be assumed that all other samples present similar underestimates of the field water content. Furthermore, considering the 1) high percentages seen in the field water content for Sample 21006, 2) the saturated percentages for 21006-2 and 21006-3 being close to the field water content of 21006, and 3) the high saturated water content percentages in the other samples, an assumption of water content at the site to be close to full saturation is therefore justifiable.

Samples originating from the same stratigraphic layer within the hut displayed similar water contents (Table 3), indicating measurement reliability (disregarding an unknown, systematic measurement or instrumentation error). Outside the hut, the water content for Layer 9 differs with a value of 85% compared to the other results from Layer 9, however this could be ascribed to possible differences in sediment packing or differences within the same layer between the inside and outside of the hut. There is of course the problem of preserving the correct packing of the sediments when measuring the saturated water contents, however, this alone cannot account for such high water content percentages. Especially when equally high values are seen in the field water content for Sample 21006, which is not affected by that problem.

The water content influences the calculation of the environmental dose rate (Table 4), given that water

present prevents grains from absorbing a higher dose of radiation (Preusser et al. 2008). There are luminescence works done in proximity to the site, where dose rates can be compared. King et al. (2013) carried out OSL dating on glacial and glaciofluvial deposits from Jostedalsbreen, northeast of Bergen, where dose rates varied between 3.18 ± 0.19 to 3.99 ± 0.24 Gy/ka. To the south of Bergen, in Sola, Selsing & Mejdahl (1994) used TL on Holocene aeolian deposits and reported dose rates of 3.24 – 4.11 Gy/ka. These comparable values reaffirm that dose rates of ~ 3 – 4 Gy/ka are possible at Nilsvikdalen, but it must also be noted that higher dose rates cannot be ruled out since this is heavily site- and water content specific. To exemplify, the bedrock at Bjorøy belongs to an area prone to have a higher background level of radon (Norges Geologiske Undersøkelse n.d.-b), which could result in high environmental dose rates present at this site.

From the calculated environmental dose rates (Table 4), values determined from the all the saturated water contents and for the field water contents of 21006-1 and 21006-2 closely resembled the dose rates reported by King et al. (2013) and Selsing & Mejdahl (1994). Even though a higher environmental dose rate is not rejected based on the water content alone, more plausible environmental dose rates are provided from the saturated values of Samples 21001 – 21005 and the field value for Samples 21006-1 and 21006-2 when considering dose rates in neighbouring regions. Additionally, accepting a higher environmental dose rate indicates the water content history to be closer to dry sediments, which is unlikely considering the site environment and morphology.

Regarding site morphology, the samples contain large quantities of sand, with all sampled layers being described as different variations of humus-rich sand containing charcoal (Åstveit et al. in prep 2022). The organic content seen from Loss on Ignition (LOI) data is ~ 4% of the samples (Appendix Table A4). Considering the water content percentages from the sandy deposits, these were all higher than first expected. To justify this, the site morphology needed more careful evaluation.

The site is described as covered in vegetation resembling a mire, while simultaneously displaying a continuous water flow in some parts of the sediment as evidenced where the uppermost layer in the stratigraphy showcases podzol processes present (Åstveit et al. in prep 2022). Previous work reports wet conditions at the site with peat covering 20 – 40 cm at the top of the sandy deposits (Kristoffersen 1995), similar to the stratigraphy seen for this site (Fig. 5). Similar stratigraphic deposits were examined in Preusser & Degering (2007), where IRSL dating of humus-rich silt deposits in between layers of peat from a mire was conducted at Niederweningen, Switzerland, where they concluded that their stratigraphy was highly saturated and reported values of 67.7 – 100.0% water content. It is thus possible to record such high water content as seen here for sandy-silty deposits with humic material present. Though not a mire, similar conditions can be argued for Nilsvikdalen: it is reasonable to assume a constant influx of water when considering the continuous precipitation known from the Bergen area. Recent records show that over the past year (2021), the month with the lowest total precipitation was May (53.5 mm), and the highest total precipitation was 641.4 mm during October – in general, the normal predictions for monthly precipitation were all between 100 – 300 mm (NRK & Meteorologisk institutt 2022). The Nilsvikdalen site is situated close to a small lake, Nordravatnet, on the north of the island (Fig. 1), and, having only smaller Quaternary deposits present above the bedrock (Norges Geologiske Undersøkelse n.d.-a) with the mentioned wet peat conditions above the sandy deposits, these conditions further support a water content close to saturation.

The different ages obtainable are plotted against the respective water content and the OSL samples placement in the stratigraphy (Fig. 14). Here, a comparison is done with the radiocarbon dates available from Åstveit et al. in prep (2022) and Halvorsen (2013). Tests were also carried out with assigning all samples the same water content percentages, for example 10, 15, 30 and 60%. From this, it could be demonstrated how, given the same water content, all samples present ages in a stratigraphically plausible order (assuming sample 21001 can be regarded as separate since it originates from outside the hut structure). This is also the case if the saturated water contents are used for 21001 – 21005 together with the field water content of 21006-2. Furthermore, the saturated water content values produce ages that are closely resembling the radiocarbon dates. Samples 21001, 21003 and 21006 display good agreement between the two dating methods, where the dates are overlapping with the corresponding ^{14}C dates within ± 1 σ. Sample 21002, 21004 and 21005 do not statistically agree with the radiocarbon dates, displaying values outside of ± 2 σ. For the samples without statistical agreement OSL ages presented are younger than the corresponding ^{14}C dates, with differences in the range of ~0.8 ka.

7.1.3 Further dose rate considerations

There are additional issues that are necessary to evaluate for the dose rate besides the water content. Since the samples were stored for approximately 10 years before being analysed, this could potentially have had an effect on age determination. Removal of the samples to a different location will possibly change the environmental dose rate the samples are exposed to during the time of storage. One might expect a lower dose rate exposure during the time of storage than for sediments exposed to the environmental dose rate *in situ*, which would alter the age determinations for the 10 years in question. It should be argued that this change will be relatively small, since 10 years in comparison to the general uncertainties of 5 – 10 % of the luminescence age itself (Duller 2008a), will be larger and thus negligible. More importantly, the water content risks being affected, as is the case for the majority of the Nilsvikdalen samples, with dried out samples as discussed above.

Additionally, the values from the ICP-MS analysis are addressed. A comparison to these can be done with data presented by Knudsen & Fossen (2001) from sand in the Jurassic Bjorøy formation and its underlying gneiss bedrock in connection to a tunnel construction at the northern part of Bjorøy, given the geographical proximity. Albeit minor, Rb can contribute to the

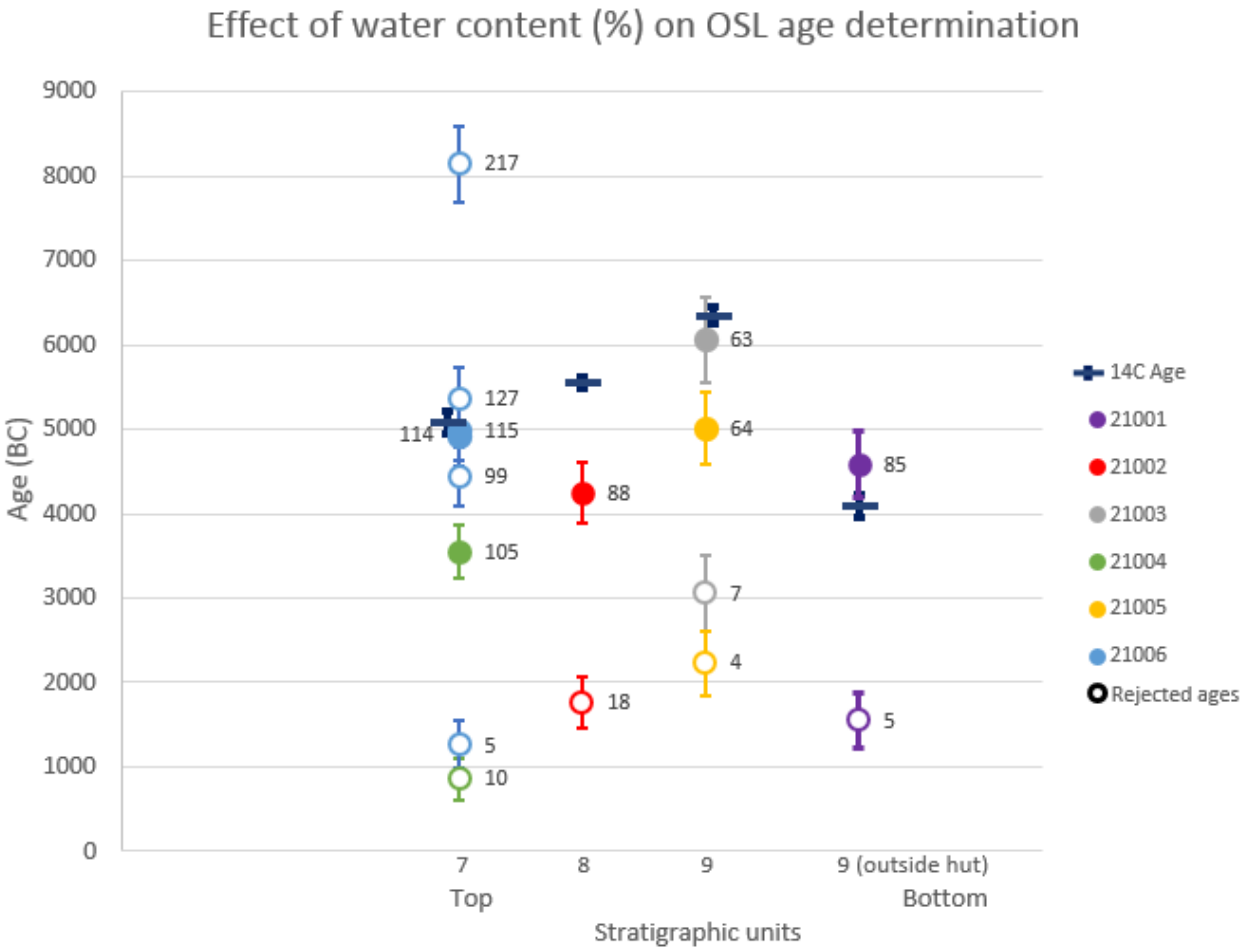

Fig. 14. Variations in water content and the resulting effect on OSL age plotted in stratigraphic order (see Fig. 5). Filled in circles are ages calculated with the chosen water contents and the hollow circles are ages calculated with rejected water contents. The water contents (%) are plotted next to their corresponding circle (see Table 4 for more details on the different calculations of saturated and field water content used). Ages are matched to their corresponding stratigraphic layers, where Layers 7 and 8 both have sampling depths of 0.65 m and Layer 9 is at 0.9 m. Radiocarbon ages are from Åstveit et al. in prep (2022), with the mean average of each time interval plotted. OSL ages are converted to years BC for the comparison.

external radiation received by the grains in addition to what K, Th and U does (Preusser et al. 2008). The sand had a Rb value of 73.91 ppm and 148.14 – 234.10 ppm for the bedrock (Knudsen & Fossen 2001). The sand value lies within the measured Rb from the ICP-MS analysis done for dose rate determination in the Nilsvikdalen 7 samples (Table 3), supporting the reliability of the Nilsvikdalen ICP-MS values.

There is also generally a possible complication of radioactive disequilibrium, i.e., changes in the radioactive decay chains leading to variations in dose rate, occurring when dealing with higher amounts of peat in the samples and if organic material is present this needs consideration for the dose rate (Duller 2008a). Since the sediments for this study resembles this scenario, with the presence of peat at the site (but not in the samples themselves) and organic material (although, as seen from LOI only up to ~ 4%, Table A4), radioactive disequilibrium could pose a potential problem. The results obtained for this study does not provide controls for whether this problem occurs and is therefore beyond the scope of this project to explore further. It is currently assumed not to be a problem for the ages seen at this site. However, future research in this region is encouraged to consider the possibilities of radioactive disequilibrium more thoroughly.

7.1.4 Age Model decision

In addition to the mean ages discussed above, ages were also obtained using the Central Age Model and the Minimum Age Model (Galbraith et al. 1999). The MAM-3 ages were significantly younger in most samples. Considering how Samples 21004 – 21006 displayed p-values (as derived from the MAM-3 model) below the desired criteria (Table 5), these ages should not be used. This is particularly important for Sample 21005, seeing as this sample was suggested for MAM-3. Overdispersion (OD) values obtained from archaeological, undisturbed, and fully bleached small aliquot samples range from 4 – 19% (with similar percentages for the medium sized aliquots) in Arnold & Roberts (2009). Compared to the OD values seen in Samples 21001 – 21006 which range from ~ 5 – 14% (Table 5) and 3.8 ± 1.1% from the dose recovery doses, this similarity confirms the samples being well bleached (other than what is seen from the D_e scatter). Another indicator of the samples being well bleached

is in the similarity in precision of the Nilsvikdalen samples and other well-bleached Scandinavian samples in Alexanderson (2022). Having well bleached samples renders the use of MAM-3 unnecessary given how it is only recommended for incompletely bleached samples (Thomsen et al. 2016), and therefore the Minimum Age Model will not be used for age determination in this case. The CAM ages were all in close agreement with the calculated mean ages (albeit slightly younger). Additionally, given how the use of CAM would only have been applicable for three of the six samples, the other three samples would still have to rely on the mean age given the excluded MAM-3 ages. Since both CAM and the mean age were in such close agreement either age model can be used; the latter was chosen in this case.

From the ages calculated from all different quartz fractions of Sample 21006, all OSL dates have a good fit with overlap within ± 1 σ of the calendar ages from the calibrated ^{14}C dates. This indicates reliable ages being possible to obtain in the case of the samples not having enough material in a specific grain size fraction, however, this is strictly site specific and needs evaluation for each new site's conditions.

7.2 Site interpretation

After having evaluated the OSL measurements, the age determinations can be interpreted archaeologically (Table 6). Calibrated ages for the archaeological periods presented below are from Bergsvik et al. (2020). Given the OSL age determinations, this places the dated cultural layer outside the hut structure in the Late Mesolithic (6500-4000 cal. BC). The bottom layer (Layer 9) inside the hut also produces Late Mesolithic dates from Sample 21005 and 21003. However, it should be noted how Sample 21003 is closer to the beginning of the Late Mesolithic than Sample 21005. The stratigraphic layer above (Layer 8) was dated to be either Late Mesolithic or Early Neolithic (4000-3300 cal. BC) (Fig. 13), with the same result for the adjacent layer (Layer 7) containing Samples 21006 and 21004. Here Sample 21006 produced an age in the Late Mesolithic. From the same layer, Sample 21004 produced an Early Neolithic age.

The placement of the hut in the Late Mesolithic to the transition into Early Neolithic supports earlier archaeological interpretations at the site (Åstveit et al. in prep 2022). With this age span, there is evidence for occupation at least during these periods (for further discussion on the archaeological evidence present, see Åstveit et al. in prep (2022)). It cannot be determined at this stage exactly when the site was abandoned for the last time, since no OSL dating took place on the overlying stratigraphic layers which also displayed traces of anthropogenic occupation. A more specific date as to when the site was first occupied is equally difficult to determine since the OSL results only date the last burial of the stratigraphic layer the sample originates from. This means in practicality that the years it took for the bottom cultural layer to form cannot be equalled to the first occasion of occupation, but rather the first date where we know with certainty that occupation was already present. (Dating of the first non-cultural layer below would have helped with bracketing the occupation age more accurately, and it is a recommendation of this research that future archaeological investigations consider this when sampling.)

It should also be briefly addressed how the radiocarbon dating and OSL dates different aspects of the site; while luminescence dating here dates the last time of exposure to light for the sediments in the cultural layers (Duller 2008a; Preusser et al. 2008), radiocarbon dating determines the time of death for the organism containing organic material (Lowe & Walker 2015). The time of death is not necessarily the same as the burial of the sediments, seeing as for example the sediments could have been exposed to light even after abandonment of the site. This, in addition to the different resolutions in age between the two dating methods, could explain some of the differences in age between the OSL and radiocarbon dates.

Table 6. Age comparisons between radiocarbon dates and OSL dates. The OSL dates are assigned archaeological periods according to the time periods in Bergsvik et al. (2020) and the stratigraphic layers with corresponding radiocarbon dates (presented as cal. Calendar ages, see Table 2) are from Åstveit et al. in prep (2022).

Stratigraphic layer	Calendar age from ^{14}C (calibrated)	Sample	OSL age (ka)	OSL age (yr BC)	Corresponding archaeological period to the OSL dates
3	220-400 AD	-	-	-	
6	4800-4610 BC	-	-	-	
7	5210-4940 BC	21004	5.56±0.32	3870-3230	Early Neolithic
		21006	6.94±0.36	5290-4570	Late Mesolithic
8	5620-5480 BC	21002	6.25±0.36	4600-3880	Late Mesolithic / Early Neolithic
9	6450-6240 BC	21003	8.07±0.51	6570-5550	Late Mesolithic
		21005	7.02±0.43	5440-4580	Late Mesolithic
9 (outside hut)	4220-3960 BC	21001	6.60±0.40	4990-4190	Late Mesolithic

7.3 Possibilities of future OSL dating at similar sites

When evaluating whether OSL dating is a viable dating method for similar archaeological sites as Nilsvikdalen, or sites such as Fosnstraumen and Ormhilleren, there are some general considerations that are worth further discussion. As Alexanderson & Murray (2012) correctly point out, regional geology plays a vital part in luminescence sensitivity, which in turn affects the precision in age determinations. They also conclude that younger samples are better dated by radiocarbon dating in terms of age precision for their specific Swedish samples. This is also the case for the Nilsvikdalen samples, that are displaying better precision for the radiocarbon dates than the OSL ages (Table 6). Having this in mind, if previous luminescence dating from the area has clearly and undoubtedly proven the area to consist of poorly dateable quartz/feldspar, and there is a possibility for radiocarbon dating, it would only be natural to rely mainly on the ^{14}C dates both regarding precision and for (potential) economic restrictions. That being said, poor luminescence qualities do not equal unusable dates, meaning luminescence dating is still a good option in cases where no other absolute dating methods are available. Further pertaining to the discussion of poor luminescence qualities, Alexanderson (2022) found how quartz originating from the Caledonian orogeny usually display poor quality; yet this is surprisingly not the case for the Nilsvikdalen quartz, despite its comparable geological origin. This needs further investigation, especially an examination of what exact conditions will affect the quartz quality and properties that make it suitable for luminescence dating. More specifically regarding the depositional environment, whether the luminescence quality may differ between geological and archaeological deposition which is currently under investigation by the Lund Luminescence Lab.

For further application of OSL dating for archaeological deposits, the condition of the site is incredibly important since it must contain the right conditions to enable luminescence dating (Fig. 15). The site needs suitable sampling conditions (where the buried layers remain sealed off from the sun and have as little bioturbation as possible) that contain quartz/feldspar grains, the sample spot needs to be situated 0.3 m below the surface (to avoid possible gamma radiation interference (Duller 2008a)) and, ideally, having clearly defined stratigraphic units (for easier connection between depositional events and ages). For further reading, both Bateman (2019) and Nelson et al. (2015) present comprehensive guides on sampling for luminescence dating.

The majority of the coastal Stone Age sites discussed by Bergsvik et al. (2020) display traces of settlements with associated artefacts, but only a reported 4% of the Early Mesolithic sites and 25% of the Middle to Late Mesolithic sites display preserved cultural layers (Bergsvik et al. 2020). In other words, many Stone Age sites will not be available for luminescence dating of specifically cultural layers, since only artefacts were found. However, seeing as ceramics too can be OSL dated as well as how burnt flint can be TL dated (Duller 2008a), luminescence dating of single artefacts is also possible. As for the sites with

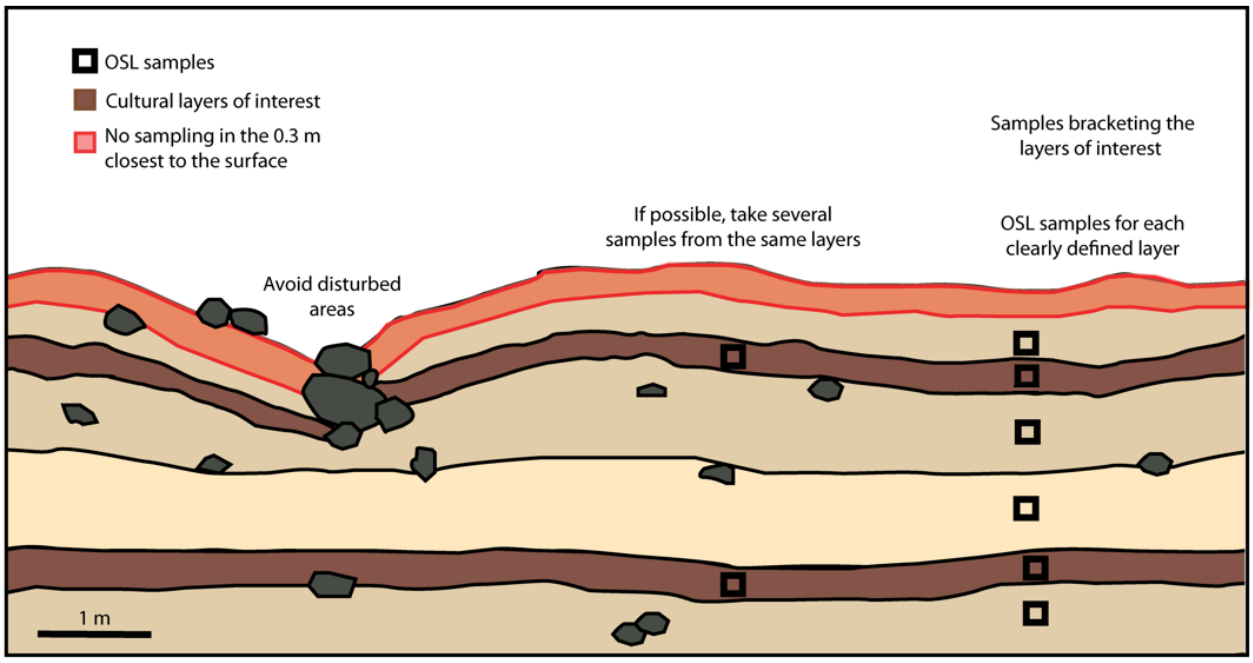

Fig. 15. Suggestions for luminescence sampling. Disturbed areas where light could have penetrated down to the sediment of interest should be avoided, likewise no sampling should be done in the top 0.3 meters. (If dating the construction of a stone structure by sampling directly below the stones, this would of course be another scenario, however, the criterion of undisturbed sediment remains.) Samples should be taken from each distinct layer and not too close to the stratigraphic unit borders, where having samples taken more or less linearly through the stratigraphy is ideal. This also helps bracket the desired stratigraphic unit's age. If possible, additional samples could be taken from other layers of interest, however analysis could be restricted due to economic issues (cost of each OSL sample and budget for the project). A more comprehensive guide to sampling is presented by Bateman (2019).

preserved cultural layers, Bergsvik et al. (2020) specifically state how there are knowledge gaps regarding the time of creation and the composition of the cultural layers found in the coastal sites. This is something OSL dating and subsequent geological evaluations of the cultural layers will be able to hopefully give more insight into.

Within this discussion, it is necessary to address possible biases in the OSL age determination process, specifically how pre-existing chronological information of the site might influence the selection and interpretation of the luminescence parameters used for the final OSL age determination. For Nilsvikdalen specifically, addressing whether having the associated radiocarbon dates available have influenced the age determination parameters chosen, and thus affected the final OSL ages is of importance. There is no denying that it is the case, thus it is important to consider if the same reasoning regarding the age determination would have occurred without the available radiocarbon dates. More importantly, it should be considered whether OSL dating can be advocated for if a comparison with other dating methods is necessary for a reliable age determination. The age determination for the six Nilsvikdalen samples was complicated owing to the complexities of the water content value. Without the site's environmental evaluation (water content history) or the comparison of dose rates and radiocarbon ages, it would undoubtedly have been more difficult to pinpoint the correct ages. Without the radiocarbon dates, this site's age determination would have culminated in ages presented in a time span of possible dates from the maximum to minimum possible ages, i.e., from the ages determined based on the field water content to those determined using the saturated water content for each sample. Considering the variation between the dry and saturated water content it would have resulted in an age difference of thousands of years, making the decision of assigning the correct archaeological periods very difficult.

However, it should not be forgotten that having the radiocarbon dates available when analysing the OSL is positive. Where sites have the possibilities of using different dating methods, the best results can be achieved through using a multitude of comparative methods and site-specific evaluations. Häggström et al. (2004) similarly concludes how the combination of several dating methods is preferable for reaching the correct ages in their study on field walls in Öggestorp, Sweden. Additionally, there is also the possibility of radiocarbon dating being unsuitable at a site. Even for OSL, there might be no problem at all with the water content, but rather with incomplete bleaching of the grains or radioactive disequilibrium. The point is how these uncertainties cannot be predicted prior to sample measurement and should not serve as a predetermined bias since all sites present different (and many times complex) dating scenarios. To eliminate such problems in the OSL age determination, simply taking a control OSL sample from a deposit of known or recent age in the nearby area to use as a comparison of the luminescence age determination components (e.g., providing a dose rate for the area which then can be used for determining parameters such as water content) would help reduce the uncertainties present in this study. In doing so, the problem of needing a comparison with (and thus having a dependency on) another dating method is reduced significantly.

Lastly, as seen from the overview of luminescence dating in Scandinavia, especially multidisciplinary studies such as Nielsen & Dalsgaard (2017) and Søe et al. (2017), there is a multitude of studies published with successful OSL dating in several different archaeological environments. For the planned future coastal Stone Age research in Vestlandet, OSL could therefore be a good alternative dating method where site conditons permits.

8 Conclusions

In this study, OSL dating has been successfully applied to cultural layers of a coastal Stone Age site at Bjorøy, Norway. The hut feature, interpreted to be broadly of Late Mesolithic age by Åstveit et al. in prep (2022), was chronometrically dated to the Late Mesolithic – Early Neolithic using luminescence dating. The OSL ages are in good agreement with the earlier site interpretation. Samples 21001, 21003 and 21006 are within ± 1 σ of the radiocarbon dates. However, Samples 21002, 21004 and 21005 are not statistically agreeing with the ^{14}C dates (ages outside of ± 2 σ), presenting younger ages than the radiocarbon dates.

The Nilsvikdalen quartz displayed good luminescence characteristics for dating, which was surprising when compared to non-archaeological quartz from the same geological origin, prompting a suggestion of future research on the conditions and properties that govern the luminescence signal. Problems with the OSL dating in this study were mainly owing to determination of the water content, since five of the six samples had dried out prior to measurement of the field water content. An extensive evaluation was undertaken to assure the correct water content was used for final age determination.

This thesis also discussed the potential of the application of luminescence dating to similar sites in future excavations. It was concluded how careful consideration of possible uncertainties, especially within the dose rate determination, must be undertaken for each individual site. Given how each site will present different complexities in age determination, both within OSL and other chronological dating methods, this study emphasises how using a multitude of comparative methods is both positive and desirable. The suggestion has been made to take a control sample of known age to reduce age determination uncertainties, as well as to compare results from different dating methods.

Where it is concluded that archaeological sites display appropriate sampling conditions, the use of OSL will indeed aid in chronological age determinations in future research. Therefore, OSL is concluded to be a good option for absolute dating of Stone Age research in Vestlandet, Norway.

9 Acknowledgements

This project would not have been possible without several people, to whom I am very grateful. My biggest and most humble thanks to my supervisors, Helena Alexanderson and Amber Hood, for their constant

support and feedback during this thesis. Thank you. I also want to thank the following: Leif Inge Åstveit (University of Bergen) for giving me the possibility to OSL date the Nilsvikdalen 7 samples and the great discussions on the site archaeology. Björn Nilsson (University of Bergen) for showing me around the coastal Stone Age sites around Bergen and the many giving discussions on the Norwegian Stone Age archaeology. Zoran Peric (Lund University) for your help with the lab work. And lastly, a thank you to my family and friends for your fantastic support and company during this project.

10 References

Aitken, M. J., 1998: *An Introduction to Optical Dating: The dating of Quaternary Sediments by the Use of Photon-stimulated Luminescence*. Oxford University Press, Oxford**.** 267 pp.

Al Khasawneh, S., Murray, A., Bonatz, D. & Freiesleben, T., 2015: Testing the application of post IR IRSL dating to Iron- and Viking-age ceramics and heated stones from Denmark. *Quaternary Geochronology 30***,** 386-391. doi: 10.1016/j.quageo.2015.05.014

Alexanderson, H., 2022: Luminescence characteristics of Scandinavian quartz, their connection to bedrock provenance and influence on dating results. *Quaternary Geochronology 69*. doi: 10.1016/j.quageo.2022.101272

Alexanderson, H. & Henriksen, M., 2015: A short-lived aeolian event during the Early Holocene in southeastern Norway. *Quaternary Geochronology 30***,** 175-180. doi: https://doi.org/10.1016/j.quageo.2015.02.014

Alexanderson, H. & Murray, A. S., 2012: Problems and potential of OSL dating Weichselian and Holocene sediments in Sweden. *Quaternary Science Reviews 44***,** 37-50. doi: https://doi.org/10.1016/j.quascirev.2009.09.020

Anjar, J., Alexanderson, H., Larsen, E. & Lysa, A., 2018: OSL dating of Weichselian ice-free periods at Skorgenes, western Norway. *Norwegian Journal of Geology 98***,** 301-313. doi: 10.17850/njg98-3-02

Arnold, L. J., Bailey, R. M. & Tucker, G. E., 2007: Statistical treatment of fluvial dose distributions from southern Colorado arroyo deposits. *Quaternary Geochronology 2***,** 162-167. doi: https://doi.org/10.1016/j.quageo.2006.05.003

Arnold, L. J. & Roberts, R. G., 2009: Stochastic modelling of multi-grain equivalent dose (D-e) distributions: Implications for OSL dating of sediment mixtures. *Quaternary Geochronology 4***,** 204-230. doi: 10.1016/j.quageo.2008.12.001

Bailey, R. M. & Arnold, L. J., 2006: Statistical modelling of single grain quartz De distributions and an assessment of procedures for estimating burial dose. *Quaternary Science Reviews 25***,** 2475-2502. doi: https://doi.org/10.1016/j.quascirev.2005.09.012

Bailey, R. M., Smith, B. W. & Rhodes, E. J., 1997: Partial bleaching and the decay form characteristics of quartz OSL. *Radiation Measurements 27***,** 123-136.

Baran, J., Murray, A. S. & Häggström, L., 2003: Estimating the age of stone structures using OSL: the potential of entrapped sediment. *Quaternary Science Reviews 22***,** 1265-1271. doi: 10.1016/S0277-3791(03)00031-3

Bateman, M. D., 2019: *Handbook of Luminescence Dating*. Whittles Publishing**.** 400 pp.

Bergsvik, K., Darmark, K., Hjelle, K. L., Aksdal, J. & Åstveit, L. I., 2021: Demographic developments in Stone Age coastal western Norway by proxy of radiocarbon dates, stray finds and palynological data. *Quaternary Science Reviews 259*, 106898. doi: 10.1016/j.quascirev.2021.106898

Bergsvik, K., Åstveit, L., Zinsli, C. & Olsen, T., 2020: *Faglig program i arkeologi for Universitetsmuseet i Bergen 2020-2025 Steinalder til og med mellomneolittisk tid (9500-2350 f.K.r.)*. University of Bergen, Bergen, Norway**.**

Bergsvik, K. A., 2001: Sedentary and mobile hunter-fishers in stone age western Norway. *Arctic Anthropology 38***,** 2-26.

Bjerck, H. 2008: Norwegian Mesolithic Trends: A Review. *In* G. Bailey & P. Spikins (eds.): *Mesolithic Europe*, 467. Cambridge University Press, Cambridge; New York.

Bondevik, S., Svendsen, J. I. & Mangerud, J., 1998: Distinction between the Storegga tsunami and the Holocene marine transgression in coastal basin deposits of western Norway. *Journal of Quaternary Science 13***,** 529-537. doi: 10.1002/(sici)1099-1417(1998110)13:6<529::Aid-jqs388>3.0.Co;2-1

Burbidge, C. I., Batt, C. M., Barnett, S. M. & Dockrill, S. J., 2001: The potential for dating the Old Scatness site, Shetland, by optically stimulated luminescence. *Archaeometry 43***,** 589-596. doi: 10.1111/1475-4754.00038

Burow, C. 2021a: calc_CentralDose(): Apply the central age model (CAM) after Galbraith et al. (1999) to a given De distribution. Function version 1.4.0. *In* S. Kreutzer, C. Burow, M. Dietze, M. C. Fuchs, C. Schmidt, M. Fischer, J. Friedrich, N. Mercier, A. Philippe, S. Riedesel, M. Autzen, D. Mittelstrass & H. J. Gray., 2021: Luminescence: Comprehensive Luminescence Dating Data Analysis. R package version 0.9.15. https://CRAN.R-project.org/package=Luminescence

Burow, C. 2021b: calc_MinDose(): Apply the (un-) logged minimum age model (MAM) after Galbraith et al. (1999) to a given De distribution. Function version 0.4.4. *In* S. Kreutzer, C. Burow, M. Dietze, M. C. Fuchs, C. Schmidt, M. Fischer, J. Friedrich, N. Mercier, A. Philippe, S. Riedesel, M. Autzen, D. Mittelstrass & H. J. Gray., 2021: Luminescence: Comprehensive Luminescence Dating Data Analysis. R package version 0.9.15. https://CRAN.R-project.org/package=Luminescence

Bøe, A.-G., Murray, A. & Dahl, S. O., 2007: Resetting of sediments mobilised by the LGM ice-sheet in southern Norway. *Quaternary Geochronology 2***,** 222-228. doi: https://doi.org/10.1016/j.quageo.2006.05.031

Bøtter-Jensen, L., Bulur, E., Duller, G. A. T. & Murray, A. S., 2000: Advances in luminescence instrument systems. *Radiation Measurements 32*, 523-528. doi: https://doi.org/10.1016/S1350-4487(00)00039-1

Chazan, M., Porat, N., Sumner, T. A. & Horwitz, L. K., 2013: The use of OSL dating in unstructured sands: the archaeology and chronology of the Hutton Sands at Canteen Kopje (Northern Cape Province, South Africa). *Archaeological and Anthropological Sciences 5*, 351-363. doi: 10.1007/s12520-013-0118-7

Degering, D. & Degering, A., 2020: Change is the only constant - time-dependent dose rates in luminescence dating. *Quaternary Geochronology 58*. doi: 10.1016/j.quageo.2020.101074

Duller, G. A. T., 2004: Luminescence dating of quaternary sediments: recent advances. *Journal of Quaternary Science 19*, 183-192.

Duller, G. A. T., 2008a: *Luminescence Dating: guidelines on using luminescence dating in archaeology*. Swindon: English Heritage.

Duller, G. A. T., 2008b: Single-grain optical dating of Quaternary sediments: why aliquot size matters in luminescence dating. *BOREAS 37*, 589-612. doi: 10.1111/j.1502-3885.2008.00051.x

Duller, G. A. T., 2018: Luminescence Analyst v.4.57. Aberystwyth Luminescence Research Laboratory, Aberystwuth University, United Kingdom.

Durcan, J. A. & Duller, G. A. T., 2011: The fast ratio: A rapid measure for testing the dominance of the fast component in the initial OSL signal from quartz. *Radiation Measurements 46*, 1065-1072. doi: 10.1016/j.radmeas.2011.07.016

Durcan, J. A., King, G. E. & Duller, G. A. T., 2015: DRAC: Dose Rate and Age Calculator for trapped charge dating. *Quaternary Geochronology 28*, 54-61. doi: 10.1016/j.quageo.2015.03.012

Eskola, K. O., Okkonen, J. & Jungner, H., 2003: Luminescence dating of a coastal Stone Age dwelling place in Northern Finland. *Quaternary Science Reviews 22*, 1287-1290. doi: https://doi.org/10.1016/S0277-3791(03)00077-5

Feathers, J. K., 2003: Use of luminescence dating in archaeology. *Measurement Science and Technology 14*, 1493-1509. doi: 10.1088/0957-0233/14/9/302

Feathers, J. K. & Bush, D. A., 2000: Luminescence dating of Middle Stone Age deposits at Die Kelders. *Journal of Human Evolution 38*, 91-119. doi: 10.1006/jhev.1999.0351

Fetter, C. W., 2014: *Applied hydrogeology. Fourth Edition.* Pearson Education, Essex. 612 pp.

Fossen, H., Mangerud, G., Hesthammer, J., Bugge, T. & Gabrielsen, R. H., 1997: The Bjoroy Formation: a newly discovered occurrence of Jurassic sediments in the Bergen Arc System. *Norsk Geologisk Tidsskrift 77*, 269-287.

Fossen, H. & Ragnhildstveit, J., 2008: Berggrunnskart Bergen 1115 I, M 1:50.000 Norges Geologiske Undersøkelse.

Fuchs, M., Kreutzer, S., Fischer, M., Sauer, D. & Sørensen, R., 2012: OSL and IRSL dating of raised beach sand deposits along the southeastern coast of Norway. *Quaternary Geochronology 10*, 195-200. doi: https://doi.org/10.1016/j.quageo.2011.11.009

Galbraith, R. F., Roberts, R. G., Laslett, G. M., Yoshida, H. & Olley, J. M., 1999: Optical dating of single and multiple grains of quartz from jinmium rock shelter, northern Australia, part 1, Experimental design and statistical models. *Archaeometry 41*, 339-364. doi: 10.1111/j.1475-4754.1999.tb00987.x

Godfrey-Smith, D. I., Huntley, D. J. & Chen, W. H., 1988: Optical dating studies of quartz and feldspar sediment extracts. *Quaternary Science Reviews 7*, 373-380.

Halvorsen, L. S., 2013: Pollen- og makrofossilanalyser fra steinalderslokaliteten Nilsvika, Bjorøy, Sund kommune, Hordaland. *Paleobotanisk rapport fra Bergen Museum, De naturhistoriske samlinger, Universitetet i Bergen 17*, 33.

Halvorsen, L. S. & Hjelle, K. L., 2017: Prehistoric agriculture in western Norway – Evidence for shifting and permanent cultivation based on botanical investigations from archaeological sites. *Journal of Archaeological Science: Reports 13*, 682-696. doi: https://doi.org/10.1016/j.jasrep.2017.05.011

Heiri, O., Lotter, A. F. & Lemcke, G., 2001: Loss on ignition as a method for estimating organic and carbonate content in sediments: Reproducibility and comparability of results. *Journal of Paleolimnology 25*, 101-110. doi: 10.1023/A:1008119611481

Hjelle, K. L., Hufthammer, A. K. & Bergsvik, K. A., 2006: Hesitant hunters: a review of the introduction of agriculture in western Norway. *Environmental Archaeology 11*, 147-170. doi: 10.1179/174963106x123188

Hood, A. G. E. & Schwenninger, J. L., 2016: Optically stimulated luminescence (OSL) dating and its applications to ancient egyptian ceramics in the 21st century. *In:* B. Bader, C. Knoblauch & E. C. Köhler (eds.) *Vienna 2: Ancient Egyptian Ceramics in the 21st Century: Proceedings of the International Conference Held at the University of Vienna 14th – 18th May 2012, OLA*.

Huntley, D. J., Godfrey-Smith, D. I. & Thewalt, M. L. W., 1985: Optical dating of sediments. *Nature 313*, 105-107.

Häggström, L., Baran, J., Ericsson, A. & Murray, A., 2004: The dating and interpretation of a field wall in Öggestorp. *Current Swedish Archaeology 12*, 43-60. doi: 10.37718/CSA.2004.03

Jacobs, Z. & Roberts, R. G., 2007: Advances in optically stimulated luminescence dating of individual grains of quartz from archeological deposits. *Evolutionary Anthropology 16*, 210-223. doi: 10.1002/evan.20150

Johnsen, T. F., Olsen, L. & Murray, A., 2012: OSL ages in central Norway support a MIS 2 interstadial (25–20 ka) and a dynamic Scandinavian ice sheet. *Quaternary Science Reviews 44*, 96-111. doi: https://doi.org/10.1016/j.quascirev.2010.10.007

King, G. E., Robinson, R. a. J. & Finch, A. A., 2013: Apparent OSL ages of modern deposits from Fabergstolsdalen, Norway: implications for sampling glacial sediments. *Journal of Quaternary Science 28*, 673-682. doi: 10.1002/jqs.2666

Knudsen, T. L. & Fossen, H., 2001: The Late Jurassic Bjoroy Formation: A provenance indicator for offshore sediments derived from SW Norway as based on single zircon (SIMS) data. *Norsk Geologisk Tidsskrift 81*, 283-292.

Kristiansen, S. M., Ljungberg, T. E., Christiansen, T. T., Dalsgaard, K., Haue, N., Greve, M. H. & Nielsen, B. H., 2021: Meadow, marsh and lagoon: Late Holocene coastal changes and human-environment interactions in northern Denmark. *BOREAS 50*, 279-293. doi: 10.1111/bor.12487

Kristoffersen, K. K., 1995: *De arkeologiske undersøkelsene på Bjorøy 1992-1994*. Arkeologisk institutt, Univ. i Bergen.

Lindvall, A., Stjern, R. & Alexanderson, H., 2017: Bleaching of quartz OSL signals under natural and laboratory light conditions. *Ancient TL 35*, 12-20.

Liritzis, I., Polymeris, G. S., Vafiadou, A., Sideris, A. & Levy, T. E., 2019: Luminescence dating of stone wall, tomb and ceramics of Kastrouli (Phokis, Greece) Late Helladic settlement: Case study. *Journal of Cultural Heritage 35*, 76-85. doi: https://doi.org/10.1016/j.culher.2018.07.009

Lowe, J., & Walker, M. J. C., 2015: *Reconstructing Quaternary Environments. Third edition (3. ed.).* Routledge/Taylor & Francis Group. 538 pp.

McEwen, L. J. & Matthews, J. A., 2013: Sensitivity, persistence and resolution of the geomorphological record of valley-floor floods in an alpine glacier-fed catchment, Leirdalen, Jotunheimen, southern Norway. *Holocene 23*, 974-989. doi: 10.1177/0959683612475144

Murray, A. S. & Clemmensen, L. B., 2001: Luminescence dating of Holocene aeolian sand movement, Thy, Denmark. *Quaternary Science Reviews 20*, 751-754. doi: 10.1016/s0277-3791(00)00061-5

Murray, A. S. & Wintle, A. G., 2000: Luminescence dating of quartz using an improved single-aliquot regenerative-dose protocol. *Radiation Measurements 32*, 57-73.

Murray, A. S. & Wintle, A. G., 2003: The single aliqout regenerative dose protocol: potential for improvements in reliability. *Radiation Measurements 37*, 377-381.

Nelson, M. S., Gray, H. J., Johnson, J. H., Rittenour, T. M., Feathers, J. K. & Mahan, S. A., 2015: User Guide for Luminescence Sampling in Archaeological and Geological Contexts. *Advances in Archaeological Practise 3 (2)*, 166-177.

Nielsen, N. H. & Dalsgaard, K., 2017: Dynamics of Celtic fields-A geoarchaeological investigation of Oster Lem Hede, Western Jutland, Denmark. *Geoarchaeology-an International Journal 32*, 414-434. doi: 10.1002/gea.21615

Norges Geologiske Undersøkelse, n.d.-a: Kart min kommune. Retrieved 2021, from geo.ngu.no/kart/minkommune/.

Norges Geologiske Undersøkelse, n.d.-b: Radon aktsomhet. Retrieved 2022-03-08, from https://geo.ngu.no/kart/radon_mobil/.

NRK & Meteorologisk Institutt, 2022: Yr - Bergen – Historikk. Retrieved 2022-03-30, from https://www.yr.no/nb/historikk/tabell/1-92416/Norge/Vestland/Bergen/Bergen?q=2021.

Preusser, F. & Degering, D., 2007: Luminescence dating of the Niederweningen mammoth site, Switzerland. *Quaternary International 164-165*, 106-112. doi: https://doi.org/10.1016/j.quaint.2006.12.002

Preusser, F., Degering, D., Fuchs, M., Hilgers, A., Kadereit, A., Klasen, N., Kreetschek, M., Richter, D. & Spencer, J. Q. G., 2008: Luminescence dating: basics, methods and applications. *Eiszeitalter und Gegenwart 57*, 95-149.

Rittenour, T. M., 2008: Luminescence dating of fluvial deposits: applications to geomorphic, palaeoseismic and archaeological research. *BOREAS 37*, 613-635. doi: 10.1111/j.1502-3885.2008.00056.x

Roberts, R. G., 1997: Luminescence dating in archaeology: From origins to optical. *Radiation Measurements 27*, 819-892. doi: 10.1016/S1350-4487(97)00221-7

Roberts, R. G., Jacobs, Z., Li, B., Jankowski, N. R., Cunningham, A. C. & Rosenfeld, A. B., 2015: Optical dating in archaeology: thirty years in retrospect and grand challenges for the future. *Journal of Archaeological Science 56*, 41-60. doi: https://doi.org/10.1016/j.jas.2015.02.028

Selsing, L. & Mejdahl, V., 1994: Aeolian stratigraphy and thermoluminescence dating of sediments of late Holocene age from Sola, southwest Norway. *23*, 92-104. doi: https://doi.org/10.1111/j.1502-3885.1994.tb00589.x

Sommerville, A. A., Hansom, J. D., Housley, R. A. & Sanderson, D. C. W., 2007: Optically stimulated luminescence (OSL) dating of coastal aeolian sand accumulation in Sanday, Orkney Islands, Scotland. *Holocene 17*, 627-637. doi: 10.1177/0959683607078987

Stroeven, A. P., Hättestrand, C., Kleman, J., Heyman, J., Fabel, D., Fredin, O., Goodfellow, B. W., Harbor, J. M., Jansen, J. D., Olsen, L., Caffee, M. W., Fink, D., Lundqvist, J., Rosqvist, G. C., Strömberg, B. & Jansson, K. N., 2016: Deglaciation of Fennoscandia. *Quaternary Science Reviews 147*, 91-121. doi: https://doi.org/10.1016/j.quascirev.2015.09.016

Søe, N. E., Ogaard, B. V., Hertz, E., Holst, M. K. & Kristiansen, S. M., 2017: Geomorphological

setting of a sacred landscape: Iron age post battle deposition of human remains at Alken Enge, Denmark. *Geoarchaeology-an International Journal 32*, 521-533. doi: 10.1002/gea.21622

Thomsen K.J., Murray, A. S., Buylaert, J. P., Jain, M., Hansen, J. H. & Aubry, T., 2016: Testing single-grain quartz OSL methods using sediment samples with independent age control from the Bordes-Fitte rockshelter (Roches d'Abilly site, Central France). *Quaternary Geochronology 31*, 77-96.

Urbanová, P., Michel, A., Cantin, N., Guibert, P., Lanos, P., Dufresne, P. & Garnier, L., 2018: A novel interdisciplinary approach for building archaeology: The integration of mortar "single grain" luminescence dating into archaeological research, the example of Saint Seurin Basilica, Bordeaux. *Journal of Archaeological Science: Reports 20*, 307-323. doi: https://doi.org/10.1016/j.jasrep.2018.04.009

Vafiadou, A., Murray, A. S. & Liritzis, I., 2007: Optically stimulated luminescence (OSL) dating investigations of rock and underlying soil from three case studies. *Journal of Archaeological Science 34*, 1659-1669. doi: 10.1016/j.jas.2006.12.004

Vervust, S., Kinnaird, T., Herring, P. & Turner, S., 2020: Optically stimulated luminescence profiling and dating of earthworks: the creation and development of prehistoric field boundaries at Bosigran, Cornwall. *Antiquity 94*, 420-436. doi: 10.15184/aqy.2019.138

Wintle, A. G., 2008: Fifty years of luminescence dating. *Archaeometry 50*, 276-312. doi: 10.1111/j.1475-4754.2008.00392.x

Wintle, A. G. & Murray, A. S., 2006: A review of quartz optically stimulated luminescence characteristics and their relevance in single-aliquot regeneration dating protocols. *Radiation Measurements 41*, 369-391.

Åstveit et al. in prep, 2022: Arkeologiske undersøkelser av steinalderboplass Lokalitet 7 Nilsvikdalen, Fjell kommune. *Arkeologiske rapporter, Fornminneseksjonen, Universitetsmuseet i Bergen, Universitetet i Bergen.* Bergen, Norway.

Appendix

Table A1: IR test of sample aliquots from 180 – 90 µm. Three aliquots were measured per sample and calculated to a mean. All samples are below 10%, where 21006 IR/B lab produced slightly higher percentages (mean 6%) than the rest.

Sample	IR/B nat	IR/B lab	Mean nat	Mean lab
21001	0%	1%	**0%**	**2%**
	0%	2%		
	0%	3%		
21002	0%	0%	**0%**	**0%**
	0%	0%		
	0%	0%		
21003	0%	0%	**0%**	**0%**
	0%	0%		
	0%	1%		
21004	0%	0%	**1%**	**1%**
	1%	1%		
	0%	1%		
21005	0%	1%	**0%**	**2%**
	0%	2%		
	1%	2%		
21006	3%	8%	**1%**	**6%**
	1%	3%		
	1%	7%		

Table A2: Dose recovery test. All samples exhibit small standard errors, as well as an accepted mean dose recovery ratio between 0.9 – 1.1 (i.e., within + 10%). Sample 21003 had one aliquot where the criteria for accepting the aliquot was not met, thus the DR ratio mean and the standard error for that sample is only calculated from two values. For sample 21006 fraction <63 µm did not pass the criteria of + 10% of the DR ratio mean, however, considering the standard error for this fraction it is within the range of passable and therefore acceptable.

Sample	Fraction (µm)	D_e (Gy)	Lab dose (Gy)	DR ratio	DR ratio mean
21001	125-180	18.82	18.49	1.02	1.04±0.02
		19.78	18.49	1.07	
		18.82	18.49	1.02	
21002	125-180	17.8	18.49	0.96	1.02±0.04
		20.16	18.49	1.09	
		18.81	18.49	1.02	
21003	125-180	16.6	18.49	0.9	0.94±0.04
		18.14	18.49	0.98	
			-	-	
21004	125-180	18.24	18.49	0.99	1.00±0.02
		18.11	18.49	0.98	
		19.32	18.49	1.04	
21005	125-180	20.25	18.49	1.09	0.95±0.07
		16.68	18.49	0.9	
		15.7	18.49	0.85	
21006	<63	19.88	18.49	1.08	1.11±0.02
		21.14	18.49	1.14	
		20.47	18.49	1.11	
21006	63-90	19.3	18.49	1.04	1.03±0.02
		18.46	18.49	1	
		19.6	18.49	1.06	
21006	90-125	19.11	18.49	1.03	1.06±0.02
		19.35	18.49	1.05	
		20.33	18.49	1.1	
21006	125-180	19.06	18.49	1.03	1.00±0.02
		17.95	18.49	0.97	
		18.35	18.49	0.99	
21006	180-250	18.78	18.49	1.02	1.02±0.02
		18.27	18.49	0.99	
		19.68	18.49	1.06	

Table A3. Bleaching test, dose measured after corresponding time exposure to natural light on a cloudy day. The percentage of the natural dose remaining is calculated against the mean D_e for 21006 (Table 5).

Time bleached (s)	Mean D_e (Gy)	Percentage of mean natural D_e (%)
5	14.33±0.80	86.7
10	9.47±0.83	57.3
15	7.30±0.67	44.2
30	3.52±0.20	21.3
60	1.68±0.07	10.2
120	0.27±0.02	1.6
300	0.12±0.01	0.7
600	0.08±0.03	0.5
1800	0.03±0.01	0.2

Table A4. Analysis of the organic content in the samples by LOI.

Sample	Weight before (g)	Weight after LOI 550 °C (g)	Weight loss (g)	Loss on ignition (%)
21001	57.14	54.74	2.40	4.20
21002	56.40	54.67	1.73	3.07
21003	56.01	54.94	1.07	1.91
21004	53.38	51.68	1.70	3.18
21005	61.18	59.18	2.00	3.27
21006	51.47	51.19	0.28	0.54

Tidigare skrifter i serien ”Examensarbeten i Geologi vid Lunds universitet”:

580. Plan, Anders, 2020: Resolving temporal links between the Högberget granite and the Wigström tungsten skarn deposit in Bergslagen (Sweden) using trace elements and U-Pb LA-ICPMS on complex zircons. (45 hp)
581. Pilser, Hannes, 2020: A geophysical survey in the Chocaya Basin in the central Valley of Cochabamba, Bolivia, using ERT and TEM. (45 hp)
582. Leopardi, Dino, 2020: Temporal and genetical constraints of the Cu-Co Vena-Dampetorp deposit, Bergslagen, Sweden. (45 hp)
583. Lagerstam Lorien, Clarence, 2020: Neck mobility versus mode of locomotion – in what way did neck length affect swimming performance among Mesozoic plesiosaurs (Reptilia, Sauropterygia)? (45 hp)
584. Davies, James, 2020: Geochronology of gneisses adjacent to the Mylonite Zone in southwestern Sweden: evidence of a tectonic window? (45 hp)
585. Foyn, Alex, 2020: Foreland evolution of Blåisen, Norway, over the course of an ablation season. (45 hp)
586. van Wees, Roos, 2020: Combining luminescence dating and sedimentary analysis to derive the landscape dynamics of the Velická Valley in the High Tatra Mountains, Slovakia. (45 hp)
587. Rettig, Lukas, 2020: Implications of a rapidly thinning ice-margin for annual moraine formation at Gornergletscher, Switzerland. (45 hp)
588. Bejarano Arias, Ingrid, 2020: Determination of depositional environment and luminescence dating of Pleistocene deposits in the Biely Váh valley, southern foothills of the Tatra Mountains, Slovakia. (45 hp)
589. Olla, Daniel, 2020: Petrografisk beskrivning av Prekambriska ortognejser i den undre delen av Särvskollan, mellersta delen av Skollenheten, Kaledonska orogenen. (15 hp)
590. Friberg, Nils, 2020: Är den sydatlantiska magnetiska anomalin ett återkommande fenomen? (15 hp)
591. Brakebusch, Linus, 2020: Klimat och väder i Nordatlanten-regionen under det senaste årtusendet. (15 hp)
592. Boestam, Max, 2020: Stränder med erosion och ackumulation längs kuststräckan Trelleborg - Abbekås under perioden 2007-2018. (15 hp)
593. Agudelo Motta, Laura Catalina, 2020: Methods for rockfall risk assessment and estimation of runout zones: A case study in Gothenburg, SW Sweden. (45 hp)
594. Johansson, Jonna, 2020: Potentiella nedslagskratrar i Sverige med fokus på Östersjön och östkusten. (15 hp)
595. Haag, Vendela, 2020: Studying magmatic systems through chemical analyses on clinopyroxene - a look into the history of the Teno ankaramites, Tenerife. (45 hp)
596. Kryffin, Isidora, 2020: Kan benceller bevaras över miljontals år? (15 hp)
597. Halvarsson, Ellinor, 2020: Sökande efter nedslagskratrar i Sverige, med fokus på avtryck i berggrunden. (15 hp)
598. Jirdén, Elin, 2020: Kustprocesser i Arktis – med en fallstudie på Prins Karls Forland, Svalbard. (15 hp)
599. Chonewicz, Julia, 2020: The Eemian Baltic Sea hydrography and paleoenvironment based on foraminiferal geochemistry. (45 hp)
600. Paradeisis-Stathis, Savvas, 2020: Holocene lake-level changes in the Siljan Lake District – Towards validation of von Post’s drainage scenario. (45 hp)
601. Johansson, Adam, 2020: Groundwater flow modelling to address hydrogeological response of a contaminated site to remediation measures at Hjortsberga, southern Sweden. (15 hp)
602. Barrett, Aodhan, 2020: Major and trace element geochemical analysis of norites in the Hakefjorden Complex to constrain magma source and magma plumbing systems. (45 hp)
603. Lundqvist, Jennie, 2020: ”Man fyller det med information helt enkelt”: en fenomenografisk studie om studenters upplevelse av geologisk tid. (45 hp)
604. Zachén, Gabriel, 2020: Classification of four mesosiderites and implications for their formation. (45 hp)
605. Viðarsdóttir, Halla Margrét, 2020: Assessing the biodiversity crisis whitin the Triassic-Jurassic boundary interval using redox sensitive trace metals and stable carbon isotope geochemistry. (45 hp)
606. Tan, Brian, 2020: Nordvästra Skånes prekambriska geologiska utveckling. (15 hp)
607. Taxopoulou, Maria Eleni, 2020: Metamorphic micro-textures and mineral assemblages in orthogneisses in NW Skåne – how do they correlate with technical properties? (45 hp)
608. Damber, Maja, 2020: A palaeoecological study of the establishment of beech forest in Söderåsen National Park, southern Sweden. (45 hp)
609. Karastergios, Stylianos, 2020: Characterization of mineral parageneses and meta-

morphic textures in eclogite- to high-pressure granulite-facies marble at Allmenningen, Roan, western Norway. (45 hp)

610. Lindberg Skutsjö, Love, 2021: Geologiska och hydrogeologiska tolkningar av SkyTEM-data från Vombsänkan, Sjöbo kommun, Skåne. (15 hp)
611. Hertzman, Hanna, 2021: Odensjön - A new varved lake sediment record from southern Sweden. (45 hp)
612. Molin, Emmy, 2021: Rare terrestrial vertebrate remains from the Pliensbachian (Lower Jurassic) Hasle Formation on the Island of Bornholm, Denmark. (45 hp)
613. Höjbert, Karl, 2021: Dendrokronologi - en nyckelmetod för att förstå klimat- och miljöförändringar i Jämtland under holocen. (15 hp)
614. Lundgren Sassner, Lykke, 2021: A Method for Evaluating and Mapping Terrestrial Deposition and Preservation Potential-for Palaeostorm Surge Traces. Remote Mapping of the Coast of Scania, Blekinge and Halland, in Southern Sweden, with a Field Study at Dalköpinge Ängar, Trelleborg. (45 hp)
615. Granbom, Johanna, 2021: En detaljerad undersökning av den mellanordoviciska ”furudalkalkstenen” i Dalarna. (15 hp)
616. Greiff, Johannes, 2021: Oolites from the Arabian platform: Archives for the aftermath of the end-Triassic mass extinction. (45 hp)
617. Ekström, Christian, 2021: Rödfärgade utfällningar i dammanläggningar orsakade av *G. ferruginea* och *L. ochracea* - Problemstatistik och mikrobiella levnadsförutsättningar. (15 hp)
618. Östsjö, Martina, 2021: Geologins betydelse i samhället och ett första steg mot en geopark på Gotland. (15 hp)
619. Westberg, Märta, 2021: The preservation of cells in biomineralized vertebrate tissues of Mesozoic age – examples from a Cretaceous mosasaur (Reptilia, Mosasauridae). (45 hp)
620. Gleisner, Lovisa, 2021: En detaljerad undersökning av kalkstenslager i den mellanordoviciska gullhögenformationen på Billingen i Västergötland. (15 hp)
621. Bonnevier Wallstedt, Ida, 2021: Origin and early evolution of isopods - exploring morphology, ecology and systematics. (15 hp)
622. Selezeneva, Natalia, 2021: Indications for solar storms during the Last Glacial Maximum in the NGRIP ice core. (45 hp)
623. Bakker, Aron, 2021: Geological characterisation of geophysical lineaments as part of the expanded site descriptive model around the planned repository site for high-level nuclear waste, Forsmark, Sweden. (45 hp)
624. Sundberg, Oskar, 2021: Jordlagerföljden i Höjeådalen utifrån nya borrningar. (15 hp)
625. Sartell, Anna, 2021: The igneous complex of Ekmanfjorden, Svalbard: an integrated field, petrological and geochemical study. (45 hp)
626. Juliusson, Oscar, 2021: Implications of ice-bedrock dynamics at Ullstorp, Scania, southern Sweden. (45 hp)
627. Eng, Simon, 2021: Rödslam i svenska kraftdammar - Problematik och potentiella lösningar. (15 hp)
628. Kervall, Hanna, 2021: Feasibility of Enhanced Geothermal Systems in the Precambrian crystalline basement in SW Scania, Sweden. (45 hp)
629. Smith, Thomas, 2022: Assessing the relationship between hypoxia and life on Earth, and implications for the search for habitable exoplanets. (45 hp)
630. Neumann, Daniel, 2022: En mosasaurie (Reptilia, Mosasauridae) av paleocensk ålder? (15 hp)
631. Svensson, David, 2022: Geofysisk och geologisk tolkning av kritskollors utbredning i Ystadsområdet. (15 hp)
632. Allison, Edward, 2022: Avsättning av Black Carbon i sediment från Odensjön, södra Sverige. (15 hp)
633. Jirdén, Elin, 2022: OSL dating of the Mesolithic site Nilsvikdalen 7, Bjorøy, Norway. (45 hp)

LUNDS UNIVERSITET

Geologiska institutionen
Lunds universitet
Sölvegatan 12, 223 62 Lund